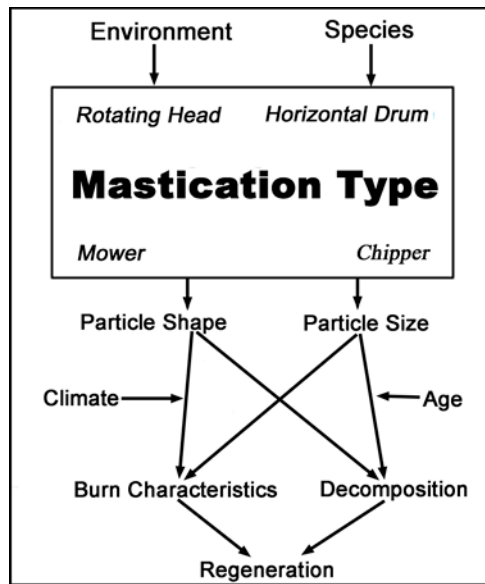# Physical and Chemical Characteristics of Surface Fuels in Masticated Mixed-Conifer Stands of the U.S. Rocky Mountains

Robert E. Keane, Pamela G. Sikkink, Theresa B. Jain

Abstract

Mastication is a wildland fuel treatment technique that is rapidly becoming the preferred method for many fire hazard reduction projects, especially in areas where reducing fuels with prescribed fire is particularly challenging. Mastication is the process of mechanically modifying the live and dead surface and canopy biomass by chopping and shredding vegetation to reduce canopy bulk density, raise canopy base height, lower surface fuelbed depth, and increase surface fuelbed bulk density, thereby reducing fire hazard. However, little is known about the properties of masticated fuelbeds as they age. In 2013, we began a comprehensive study called MASTIDON (MASTIcated fuelbed Decomposition Operational Network) to measure the diverse characteristics of masticated fuelbeds at treatment sites of different ages across the western U.S. Rocky Mountains. Our primary objective was to evaluate effects of aging of masticated fuelbeds on fire behavior, fuel moisture dynamics, soil heating, and smoldering combustion. Results from these investigations could then be used to build fire behavior fuel models for use in operational fire management. This report concerns a small facet of the MASTIDON study, where summaries of the physical and chemical fuel properties of the sampled masticated fuelbeds are presented and the relationships of these properties to fuel age are explored. We document masticated fuelbed characteristics and correlate these characteristics to age. In general, we found that there were few changes in physical and chemical properties over the short 10 years represented by the sites in this study, primarily due to confounding factors of low decomposition rates, diverse mastication techniques, wide range of biophysical conditions, and high variability in fuel properties across disparate sites. However, we feel it will take more than 10 years for decomposition to mitigate the negative impacts of wildfires burning in masticated fuelbeds. These summaries can be used to understand how different types of masticated fuelbeds might burn if ignited and as inputs to fire behavior and effects models.

Keywords: mastication, ponderosa pine, fuel treatment, wildland fuel properties, fuel layers, fuel particles

The Authors

Robert E. Keane is a Research Ecologist with the U.S. Forest Service, Rocky Mountain Research Station (RMRS) at the Missoula Fire Sciences Laboratory in Missoula, Montana. His most recent research includes (1) developing ecological computer simulation models for exploring landscape, fire, and climate dynamics; (2) sampling, describing, modeling, and mapping fuel characteristics; and (3) investigating the ecology and restoration of whitebark pine. He received a B.S. degree in forest engineering from the University of Maine, Orono; an M.S. degree in forest ecology from the University of Montana; and a Ph.D. in forest ecology from the University of Idaho.

Pamela G. Sikkink is a postdoctoral Research Biologist with U.S. Forest Service, Rocky Mountain Research Station (RMRS). She is employed with the Forest and Woodland Ecosystems program in Moscow, Idaho, but stationed with the Missoula Fire Sciences Laboratory in Missoula, Montana. Her most recent research includes (1) sampling and describing masticated fuels, (2) evaluating methods of describing fire and burn severity, (3) sampling and describing grassland fuels, and (4) testing sampling methods for long-term vegetation monitoring in Yellowstone National Park. She received a B.S. degree in biology and geology from Bemidji State University in Minnesota, master's degrees in geology and forestry from the University of Montana, and a Ph.D. in forestry from the University of Montana.

Theresa B. Jain is a Research Forester in the U.S. Forest Service, Rocky Mountain Research Station (RMRS), Forest and Woodland Ecosystems program in Moscow, Idaho. Her research expertise is in silviculture and fuels. Currently her research focuses on developing, implementing, and evaluating alternative silvicultural management strategies for addressing integrated fuel treatment and restoration objectives in moist and dry mixed-conifer forest. She has developed and installed integrated fuel treatment landscape studies at Boise Basin and the Black Hills Experimental Forests, both of which occur within dry mixed-conifer forests. She earned a B.S. degree in forest management, an M.S. degree in silviculture with an emphasis on soil processes, and a Ph.D. in silviculture with an emphasis on landscape ecology and applied statistics, all from the University of Idaho.

Acknowledgments

Contents

1. Introduction

Wildland fuel "mastication" has been used for some fire hazard reduction projects since the 1950s (Lambert and McCleese 1977; Pokela 1972; Ritter 1950), but only recently has it become a popular method for fuel treatments in the United States. (Harrod et al. 2009; Stephens et al. 2012). Fuel mastication has been defined in several ways (Harrod et al. 2009; Rummer 2006). In this paper, we define mastication as the process of mechanically modifying live and dead surface and canopy biomass to reduce fire hazard by lowering fuelbed depth, increasing surface layer bulk density, and raising canopy base height (Kreye et al. 2014a). Today there are many methods and techniques for masticating fuels, including chipping, grinding, flailing, and cutting (Harrod et al. 2009; Jain et al. 2012; McKenzie and Makel 1991). This variety of methods and the low risk of harm to humans, make mastication a popular choice for a fuels treatment technique across many land management agencies and locations (Halbrook et al. 2006). In many areas of the wildland-urban interface, mastication may be the only alternative for reducing canopy fuels because prescribed burning treatments may pose greater threats to adjacent properties and commercial thinning may be a difficult and cost-prohibitive approach (Berry and Hesseln 2004).

Although research on this newly popular treatment is limited, there has been work on its implementation and effects. Halbrook et al. (2006) and Jain et al. (2012) reviewed available techniques, their application, and associated costs. The effects of mastication on fuel moisture dynamics were studied by Kreye and Varner (2007) and Kreye et al. (2012). Effects on soil properties were assessed by Busse et al. (2006). The effects of fire behavior (Bradley et al. 2006; Glitzenstein et al. 2006; Smith and Brewer 2011), soil heating (Busse et al. 2005), smoke production (Achtemeier et al. 2006; Naeher et al. 2006), and vegetation responses (Battaglia et al. 2006) were evaluated when masticated fuelbeds burned in the laboratory. Impacts of mastication on soil processes (Busse et al. 2006; Windell et al. 1986), vegetation development (Battaglia et al. 2006), and wildlife habitats (Moreno-Fernández et al. 2016) have been used to guide design of concurrent treatments for fuels management, ecosystem restoration, rehabilitation, or wildlife management. A major finding from many of these studies is that understanding effects of mastication on fuelbed characteristics and resultant fire behavior is critical to fire management because most adverse effects of mastication are from unplanned burning in wildfires (Smith and Brewer 2011). Given the diversity of mastication methods (Jain et al. 2012; Rummer 2006) and the high variability of fuel and microsite conditions within treated stands (Battaglia et al. 2010; Kane et al. 2006; Keane et al. 2012a), the impacts of mastication may be quite complex and highly variable. Any investigation into mastication effects must account for variations due to mastication technique, mode of implementation, and spatial variability of fuelbed characteristics before and after treatment (Jain et al. 2012; Keane et al. 2012a).

One major aspect of mastication that has not been well studied is the changes that occur as masticated fuelbeds age (Brennan and Keeley 2015; Kreye et al. 2014a, 2016). Newly masticated fuelbeds (less than 3 years) consist of amorphous chopped or crushed woody pieces that have sharp edges with higher surface area (Knapp et al. 2008). Initially, moisture contents of woody particles may be high, but subsequent drying increases the likelihood that these fuels will ignite easily and carry flames across a forest

stand (Knapp et al. 2011). However, as masticated fuel particles age, the litter and fractured wood particles decompose, resulting in major changes in both particle and fuelbed characteristics, such as reductions in particle density, fuel loadings, and fuelbed depth (Keane 2015). Relatively little is known about how structural, physical, and chemical characteristics of masticated fuel particles change over time and how these changes affect fuelbed moisture dynamics and fire behavior. Kreye et al. (2016) explored the effects of aging on fire behavior and Battaglia et al. (2015) looked at changes in soil nitrogen and loading, but neither investigated changes in particle properties. Of special concern to fire managers is whether the properties of the masticated fuel change so much that new fire behavior fuel models are needed to simulate fire behavior (Knapp et al. 2008; Kreye et al. 2014a). Even more important is how temporal changes in masticated fuelbed properties will influence future fire effects if the masticated stand burns, such as smoke production, soil heating, and ecological responses to these novel fuel conditions (Busse et al. 2006).

In 2013, we initiated a comprehensive study called MASTIDON (MASTIcated fuelbed Decomposition Operational Network) to evaluate fire behavior, fuel moisture dynamics, soil heating, and smoldering combustion of different aged masticated fuelbeds. Critical to MASTIDON objectives was the measurement of the diverse physical and chemical characteristics of masticated particles, fuel layers, and fuelbeds to provide context for understanding changes in masticated fuelbed fire behavior and other important management considerations (Battaglia et al. 2006, 2015). Masticated fuelbed and particle properties measured in MASTIDON were correlated with variables that represent fire behavior, moisture, and smoldering combustion dynamics (Sikkink et al., 2017), and more importantly, the properties were used to evaluate fire behavior fuel models for application in masticated fuelbeds during operational fire management (Knapp et al. 2008; Kreye et al. 2014a; Scott and Burgan 2005). This report presents a small but important part of the MASTIDON project: the detailed summaries of the changes in physical and chemical fuel properties over 10 years represented in this study using field collections from different aged masticated fuelbeds across the U.S. Rocky Mountains.

1.1. Background

As mentioned, mastication involves cutting, chopping, or mulching live trees, shrubs, and herbaceous fuels and depositing the manipulated material on the ground (Harrod et al. 2009; Jain et al. 2012). Mastication can be combined with many silvicultural activities, such as commercial and noncommercial thinning, and it can also be integrated with prescribed burning to consume flashy fuels, reduce heavy surface fuel loadings, and kill small saplings (Reiner et al. 2009; Weed et al. 2015). A variety of mastication methods can be used to mechanically manipulate canopy and surface vegetation, and the individual method will dictate the amount, spatial distribution, and properties of masticated fuel (Jain et al. 2012; Keane et al. 2012b).

1.1.1 Mastication Mechanical Configurations

The types of equipment used to masticate forests and shrublands are as diverse as the fuel particles they create (Jain et al. 2012; Windell and Bradshaw 2000). Mastication equipment is used to lop and scatter, cut and trample, crush, chop, or cut brush, or shred most types of live and dead biomass, especially shrubs, saplings, and pole-size trees up to 30 inches (76 cm) in diameter, depending on the power of the cutting head (Vitorelo et

Table 1—Characteristics of vertical- and horizontal-shaft brush-cutting heads (Coulter et al. 2002; Forests and Rangelands 2015; McKenzie and Makel 1991; Rummer 2009; Vitorelo et al. 2009; Windell and Bradshaw 2000).

Vertical-shaft	Horizontal-shaft
Head and cutting attachments	
Cutting devices are attached to a disk or robust mowers	Cutting devices attached to a horizontal shaft or drum
Fixed teeth or blade (mower type)	Fixed teeth, swinging hammers, or ax/knife blade
Boom or front-end mounted	Boom or front-end mounted
Vegetation best suited to treat	
Slash and shrubs	Slash, shrubs when front end mounted
Trees 6 to 8 inch diameter when boom mounted	Trees up to 30 inches diameter when boom mounted
Piece size and posttreatment condition	
Creates large pieces (chunks or shredded)	Creates small pieces
Leaves ragged stumps	Leaves clean cut stumps
Carrier Machines	
Excavator, skid steer, tractors (hydraulic and power take-off)	Excavator, skid steer, tractors (hydraulic and power take-off)
Micro-topography	
Broken or dissected topography with a diversity of slope angles and aspects	Continuous slopes that have similar slope angles and aspects

al. 2009). Further, the type and size of biomass (shrubs or trees), physical setting, cutting head, carrier machine, location of mounting (boom or front-end), and the operator can greatly influence the characteristics of the post-mastication fuelbed (Jain et al. 2012).

There are two general types of cutting heads: vertical and horizontal shaft (table 1, figs. 1a and 1b). A vertical shaft head is a disk or robust mower that can have either fixed teeth (fig. 1a and fig. 1b), swinging hammers (fig. 1c), and swinging knives (fig. 1d). Vertical shaft heads are best suited to masticate shrubs and trees 6 to 8 inches (15 to 20 cm) in diameter when boom mounted. They often create wood chunks, shredded woody pieces, and ragged stumps. They can be mounted on excavators, skid steers, and tractors, and they work best in broken or dissected topography.

In contrast, horizontal shaft heads are attached to a drum, which can be either front-end (figs. 1b, 1d, 1e) or boom mounted (figs. 1a, 1c) This type of head can treat shrubs and trees up to 76 cm (30 inches) in diameter when boom mounted and creates small pieces and wood chips while leaving clean-cut stumps. It can be mounted on all three types of machines and is best used on flatter slopes with less dissected conditions. The slope threshold and extent of soil disturbance can vary depending on the carrier machine and where the cutting head is mounted. For example, tracked excavators can work with wider strips and tend to have less soil disturbance with a boom-mounted masticating head than with a front-end mounted masticating head (Rummer 2006).

In addition to masticators, self-propelled whole-tree chippers that are equipped with a shear blade may be used to treat standing trees and shrubs and spread the chips within the stand when there is lack of hog or biofuel infrastructure (Harrod et al. 2009). This equipment works best on flat ground and on slopes less than 30 percent. Whole-tree chippers are primarily used for cutting and chipping trees and treating post-harvest slash (fig. 1f).

Figure 1—There are two primary equipment types most commonly used for mastication (also referred to mulching) treatments. Cutting tools placed on either a (a) vertical shaft (photo from amacocei.com) or (b) horizontal shaft (photo from txbrushcutter.com) using different configurations such as (c) fixed teeth, swinging hammers (photo from rockhound.com) and (d) swinging knives (photo from forestfireequipment.com). Carrier machines include skid steers, excavators and tractors and cutting heads can either be boom- (a and c) or front-end (b, d, and e) mounted. Tools for wood chipping are also commonly used. (e) Skid steer with flail cutter attached to front (photo from bobcat.com) and (f) drum-chipper (photo morbark.com).

Unlike masticators, they contain a chipping head and material must be fed into the chipper; some machines, such as the Mountain Goat chipper (Marbark LLC, Winn, MI) used in our study, can have a shear attached to the machine (fig. 1f). Wood chip size and thickness often depend on the density and size of the biomass. Other types of self-propelled chippers require a separate machine to cut the trees and slash and feed the chipper.

In the MASTIDON study, the sites we sampled were treated using one of four distinct types of mastication tools: (1) mounted horizontal shaft (fig. 1b), (2) boom-mounted vertical shaft (fig. 1a), (3) chipper (fig. 1f), and (4) mounted vertical shaft with free-swinging cutters (similar to a mower) (fig. 1e). We use the term "mastication method" (MAST) to describe these four types of equipment configurations.

1.1.2 Physical Characteristics

Physical characteristics of masticated fuelbeds are those variables that describe size, shape, weight, and density. In this study, physical properties were measured at three scales: particle, layer, and fuelbed (Keane 2015). Particle scale, three-dimensional variables were often summarized to describe fuel layer and fuelbed variables and to calculate other physical characteristics important to fire science; these measurements included length, width or diameter, and height. Particle length is the maximum distance between the two particle ends; most natural fuel particles are branches or twigs, so the length is the distance between the two semi-round ends. However, most masticated fuel particles are broken shards of wood, so the length is the longest axis. Width is the greatest distance across a fuel particle; for intact branches and twigs, the width is also the diameter. Width is often measured perpendicular to the length. Height is the third measurement only for masticated wood particles; it is the remaining dimension to be measured when there is no detectable diameter. Based on these dimensions, we also summarized characteristics by three size categories named for their moisture time lag: (1) 1-hr fuels are 0.0 to 0.25 inches (0 to 6 mm) in diameter or width, (2) 10-hr fuels are 0.25 to 1.0 inches (6 to 25 mm) in diameter or width, and (3) 100-hr fuels are 1.0 to 3.0 inches (25 to 76 mm) in diameter or width (Keane 2015).

Masticated fuel particles occur in all shapes. The three-dimensional variables (length, width, height), along with an approximated shape, are often used to compute particle volume. Volume is then used with particle mass to compute particle density (i.e., wood density or specific gravity). Surface area and surface-area-to-volume ratio (SAVR), which are the most important characteristics used in conventional fire modeling (Rothermel 1972), are also estimated from dimensional and shape measurements.

Two types of densities are often used to describe fuelbed properties: particle density and bulk density. They are expressed in the same units (g or kg dry mass m^{-3}) but are fundamentally different in interpretation (Keane 2015). Particle density is the dry mass per unit volume of a solid fuel particle, such as a twig, piece of bark, or log. Bulk density is the dry mass per unit volume of a fuel layer (shrub, herb), component (litter, duff, fine woody debris), or entire fuelbed. The primary difference is that bulk density includes all air voids within the volume whereas particle density is specifically for a solid piece of fuel.

In this study, we defined the masticated fuelbed as all surface fuels that are above the mineral soil surface to the height of 2 m (Keane 2015). We stratified the masticated fuelbed into five distinct layers (fig. 2). The fresh litter layer contains all the dead biomass

Figure 2—Cross-sectional view of the masticated fuelbed illustrating the five distinct layers identified in this project.

that has fallen on the fuelbed since mastication, such as needles, cones, leaves and flowers, seeds, reproductive parts, and roots. Under fresh litter is the masticated layer, which includes all the new fuels that have been deposited by the mastication treatment plus all surface fuels present prior to the treatment. The third layer, masticated-duff, contains masticated fuels mixed with duff and the natural fuels on the ground prior to treatment. This layer is often created by machine-transport mixing during the mastication treatment and through physical (soil movement, freezing and thawing) and biological (micro- and macro-organism movement) processes over time. The duff layer includes all the unaltered decomposed material below the masticated layer. Duff is separated from other fuels by using the criteria provided in Keane (2015). The origins of the decayed duff material cannot be determined; in contrast, the origins of masticated material (e.g., wood, needles, buds) can easily be recognized. Often there is also a fifth layer, the duff-soil layer, in masticated fuelbeds because of the effects of machinery trampling; mineral soil becomes incorporated into the duff layer as vehicle tires or tracks dig into the ground. This layer differs from the others because of its high mineral content, which can dampen fire behavior and highly influence smoldering combustion (Hatten and Zabowski 2010; Philpot 1970). In some of our older masticated units there were shrub and herb layers above the masticated fuelbed, but they were ignored in our analysis because they had low biomass relative to masticated fuels. Logs were rare in our study sites, and although they were sampled in the MASTIDON effort, they are ignored in this report.

1.1.3 Chemical Characteristics

Chemical characteristics describe important elements in the chemical composition of the fuel that may affect fire behavior and decomposition. Lignin and cellulose contents often correlate with the stage of decomposition of a fuel particle (Keane 2015). Newly deposited particles have higher proportions of cellulose than particles with advanced decomposition, which usually have high lignin contents that make them more likely to smolder. Chemical changes that woody fuel particles undergo as they decompose over time are closely related to the physical changes that occur in the fuelbed. Loss of cellulose and lignin within the wood cells results in a loss of structural integrity. As cellulose and lignin in the wood particles degrade, fuelbed characteristics (such as bulk density, particle packing, porosity, particle shape, moisture retention, and mass) decrease (Duryea

et al. 1999). Quantifying this degradation process is the rationale for conducting cellulose and lignin tests in the MASTIDON study. Heat content was assigned as a chemical characteristic because it is related to how we measured lignin and cellulose content (see section 2.3.3.2).

Carbon and nitrogen contents, and their ratio, may also be used to describe the stage of decomposition of woody fuel. Newer fuels have higher nitrogen concentrations (Harmon et al. 1986), but as fuels age, the nitrogen is often used by microbes in the decomposition process or leaches into the soil. Carbon is also lost as microbes consume cellulose and other structural carbon (Harmon et al. 1986).

1.2 Study Objectives

As mentioned, the subject of this report is a description of the physical and chemical properties of masticated fuelbeds and how these properties change over time. The primary objective was to describe fuelbed characteristics for masticated fuels of different ages by structural, physical, and chemical attributes. These attributes could be important in understanding changes in fire behavior and effects as masticated fuelbeds age.

Information from this effort was used in all other phases of the MASTIDON project, but it also has great value on its own to fire scientists and managers. Findings from this study may provide important parameters to use in other fuel modeling, sampling, and mapping efforts (Pan et al. 2011). Woody fuel particle structural characteristics can be used to estimate loading, for example, and chemical characteristics can be used as parameters in ecosystem models to simulate fuel decomposition (Keane 2015).

2. Methods

A fuelbed scaling hierarchy was created to facilitate efficient description and quantification of masticated fuelbed properties and compositions (table 2). Within each of the five masticated fuelbed layers (fig. 2), we created finer scales to best describe variables that we sampled in the field or estimated in the laboratory. However, due to time and funding constraints, we could not measure all variables at every hierarchical scale. Therefore, we concentrated most of the physical and chemical measurements on only those variables that described the masticated fuel layers and particles (table 3). When possible, we used summaries of variables at finer scales to estimate variables at the coarser scales.

Table 2—Scales of masticated fuelbeds used in this study, listed by increasingly fine levels of measurements used to describe the entire masticated fuelbed.

Scale	Description	Number
Macroplot	The 50 m by 30 m rectangular macroplot used to bound field measurements (fig. 5).	1
Grid point	A point within the 50x30 m grid placed at 3 m intervals along 30 m transects established at 10 m intervals along the 50 m baseline (fig. 5).	66
Transect	A 30 m linear line used to establish grid points or microplots, and also used to sample log (>12 cm diameter) loading using planar intersect methods.	6
Microplot	The 1 m^2 sampling frame used for destructive field sampling to describe the fuel characteristics presented in this report.	20
Fuel layer	The masticated fuelbed consists of five major layers in this report. These include fresh litter, masticated woody, mixed masticated woody and duff, duff, and mixed duff and mineral soil (fig. 2).	5
Size class	Woody masticated fuel was separated into three standard size classes based on particle diameter: 0-6 mm (1-hr fuels), 0.6-25 mm (10-hr fuels), and 25–76 mm (100-hr fuels).	3
Shape	All woody masticated fuel was also separated into 13 shape classes that are described in table 5.	13
Particle	Organic woody particles within each layer were measured for size and weight, described for surface characteristics, tested for moisture-loss patterns, and pulverized for chemical analyses.	many

Table 3—Field-sampled and calculated variables recorded at each of the 15 sample sites at various fuelbed scales (table 2). Three general methods were used: M = measured, VE = visual estimate, C = calculated. NA = not applicable. Sample sites are listed in table 4.

Scale	Method	Description	Unit
Macroplot		**A 30 m by 50 m rectangular plot installed in a representative area within treated unit (fig. 5)**	
	M	Location of the lower left corner of the grid in Universal Transverse Mercator (UTM)	m
	NA	Digital photo of plot	NA
	M	Elevation	m
	M	Slope	decimal degree
	M	General aspect	degree azimuth
Grid point		**A point in a grid installed within the macroplot (fig. 5)**	
	M	Fresh litter layer depth	cm
	M	Masticated layer depth	cm
	M	Duff-masticated layer depth	cm
	M	Duff layer depth	cm
	M	Duff-soil layer depth	cm
	VE	Grass loading (visual estimate of material in 1-m2 area surrounding grid point)	Percent cover
	VE	Shrub loading	Percent cover
	VE	Forb loading	Percent cover
	M	Vegetation list by common names and species (if known)	NA

| Scale	Method	Description	Unit
Microplot		**A 1 m by 1 m square fixed area plot used to sample fine scale fuel attributes and placed at 20 points within the macroplot (fig. 5)**	
	M	North grid point UTM coordinate	m
	M	East grid point UTM coordinate	m
	NA	Digital photos of microplot (full and ¼ H-W section)	NA
	M	Fuel layer depths for each corner of microplot and H-W section	cm
	C	Loading or mass per unit area	kg m^{-2}
	C	Bulk density of fuelbed	kg m^{-3}
	C	Mineral content of duff layer	percent
Fuel Layer		**A distinct layer in the fuel vertical profile that is important for understanding mastication effects – there are five major layers**	
	M	Depth of layer	cm
	C	Loading or mass per unit area	kg m^{-2}
	C	Bulk density of fuel layer	kg m^{-3}
Shape	NA	**The general shape of a masticated woody fuel particle**	
	M	Shape category of masticated fuels only	class
	M	Dry weight of particles by shape	g
	M	Chemical content for four masticated particle shapes (cylinder, triangle, parallelogram, wood chips)	percent
	M	Heat content	percent
	M	Cellulose fraction dry weight for four masticated particle shapes (cylinder, triangle, parallelogram, wood chips)	percent
	M	Lignin fraction dry weight for four masticated particle shapes (cylinder, triangle, parallelogram, wood chips)	percent
	M	Nitrogen concentration dry weight for four masticated particle shapes (cylinder, triangle, parallelogram, wood chips)	percent
	M	Carbon fraction dry weight for four masticated particle shapes (cylinder, triangle, parallelogram, wood chips)	percent
	C	Carbon:Nitrogen ratio for four masticated particle shapes (cylinder, triangle, parallelogram, wood chips)	dimensionless
Size class		**The standard size classes (1, 10, 100, 100 hr) of masticated woody fuels only**	
	M	Count of total number of particles in each shape and size class	Number m^{-2}
	M	Total fuel load of particles by size class (wet weight)	g
	C	Total fuel load of particles by size class (dry weight)	g
	M	Dry weight of particles by size class (subsample only)	g
	M	Percent moisture by size class (subsample only)	percent
	M	Chemical content for 1-hr, 10-hr, and 100-hr size classes of the masticated particle shapes (cylinder, triangle, parallelogram, wood chips)	percent
	M	Heat content	percent
	M	Cellulose fraction dry weight	percent
	M	Lignin fraction dry weight	percent
	M	Nitrogen concentration dry weight	percent
	M	Carbon fraction dry weight	percent
	C	Carbon:Nitrogen ratio for only masticated particles	ratio
Particle		**Any intact or fragmented piece of masticated woody fuel**	
	M	Dry weight	g
	M	Particle shape (see table 5)	class
	M	Longest length of fuel particle	cm
	M	Width or diameter of particle	cm
	C	Surface area	cm^2
	C	Volume	cm^3
	C	Surface area:volume ratio	cm^{-1}
	M	Particle description (hardness, bark and soil characteristics, end description, surface texture, alterations, color, and porosity estimate)	NA
	M	Particle density	gm cm^{-3}

2.1 Study Sites

We used a spatial chronosequence approach in this study to represent different fuel ages where we sampled 15 study sites in two types of mixed coniferous forests of the Rocky Mountains that represented seven "treatment" ages (years after treatment) (table 4). Selection of sample sites was restricted to certain treatment areas because we needed a variety of: (1) treatment ages; (2) mastication methods; (3) mature, mixed-conifer stand types; and (4) geographic areas within the Rocky Mountains. After contacting numerous agencies and fire managers, we found only 15 sites that met these criteria that we could feasibly sample, process, and analyze within the 2 years allotted to this study (table 4).

Most of our sites (11) were composed mainly of ponderosa pine (*Pinus ponderosa*) or mixed ponderosa pine and Douglas-fir (*Pseudotsuga menziesii*) stands; all were on relatively flat ground (fig. 3). Climates were generally semi-moist to dry based on annual rainfall, which was often less than 40 cm yr^{-1}. Sites were spread from northern Idaho

Table 4—Characteristics of study sites sampled in the MASTIDON project. Tree species include ponderosa pine (PP), Douglas-fir (DF), western hemlock (WH), western larch (WL), western white pine (WWP), and western red cedar (WRC). Locations: six experimental forests (EFs), one national forest (NF), and one national preserve (NP) in either the PP or PP/DF stands (dry) or the moist mixed-species stands (moist). MAST used these machines: horizontal shaft (HS) and vertical shaft (VS) that have either fixed teeth (FT) or swinging knives (SK) and were boom mounted (BM) or front-end mounted (FEM) with or without a rotating head (RH).

Location	Name	Mixed-conifer climate type	Dominant species	Treatment date	Age of materials (yrs)	Mastication method (MAST)
Boise Basin EF, Idaho	Amber	Dry	PP	2004	10	VS, FT, BM (=RH)
Boise Basin EF, Idaho	AmberNew	Dry	PP, DF, *Purshia tridentata*, *Symphoricarpos albus*	2010	4	VS, FT, BM (=RH)
Black Hills EF, South Dakota	BHMix	Dry	PP, *Arctostaphylos uva-ursi*	2012	2	VS, SK, FEM (Mowed)
Black Hills EF, South Dakota	BHMow	Dry	PP, *Arctostaphylos uva-ursi*, *Symphoricarpos albus*	2012	2	VS, SK, FEM (Mowed)
Deception Creek EF, Idaho	DC1	Moist	WH, WWP, WL, *Linnaea borealis*	2004	9	VS, FT, BM (=RH)
Manitou EF, Colorado	MEFChip	Dry	PP, DF, *Symphoricarpos albus, Juniperus communis*	2004	10	Chipped
Manitou EF, Colorado	MEFWS	Dry	PP, DF, *Arctostaphylos uva-ursi*	2005	9	VS, FT, FEM (=RH)
Priest River EF, Idaho	PR3	Moist	WRC, WH, WWP, WL	2011	2	HS, FT, FEM
Priest River EF, Idaho	PRCC1	Moist	WWP, WH, WL, *Clintonia uniflora*	2007	6	VS, FT, BM (=RH)
San Juan NF, Colorado	Skelton	Dry	PP, DF, *Artemisia tridentata*	2010–2011	3	VS, FT, FEM (=RH)
Santa Fe NF, New Mexico	LG	Dry	PP, bunchgrass	2006	8	HS, FT, FEM
Santa Fe NF, New Mexico	PAL	Dry	PP, sedge	2011–2012	2	HS, FT, FEM
University of Idaho EF, Idaho	UI	Moist	PP, *Physocarpus malvaceus*	2014	0	HS, FT, BM
Valles Caldera NP, New Mexico	VC1	Dry	PP, sedge, bunchgrass	2007–2008	6	HS, FT, FEM
Valles Caldera NP, New Mexico	VC2	Dry	PP, bunchgrass	2012	2	HS, FT, FEM
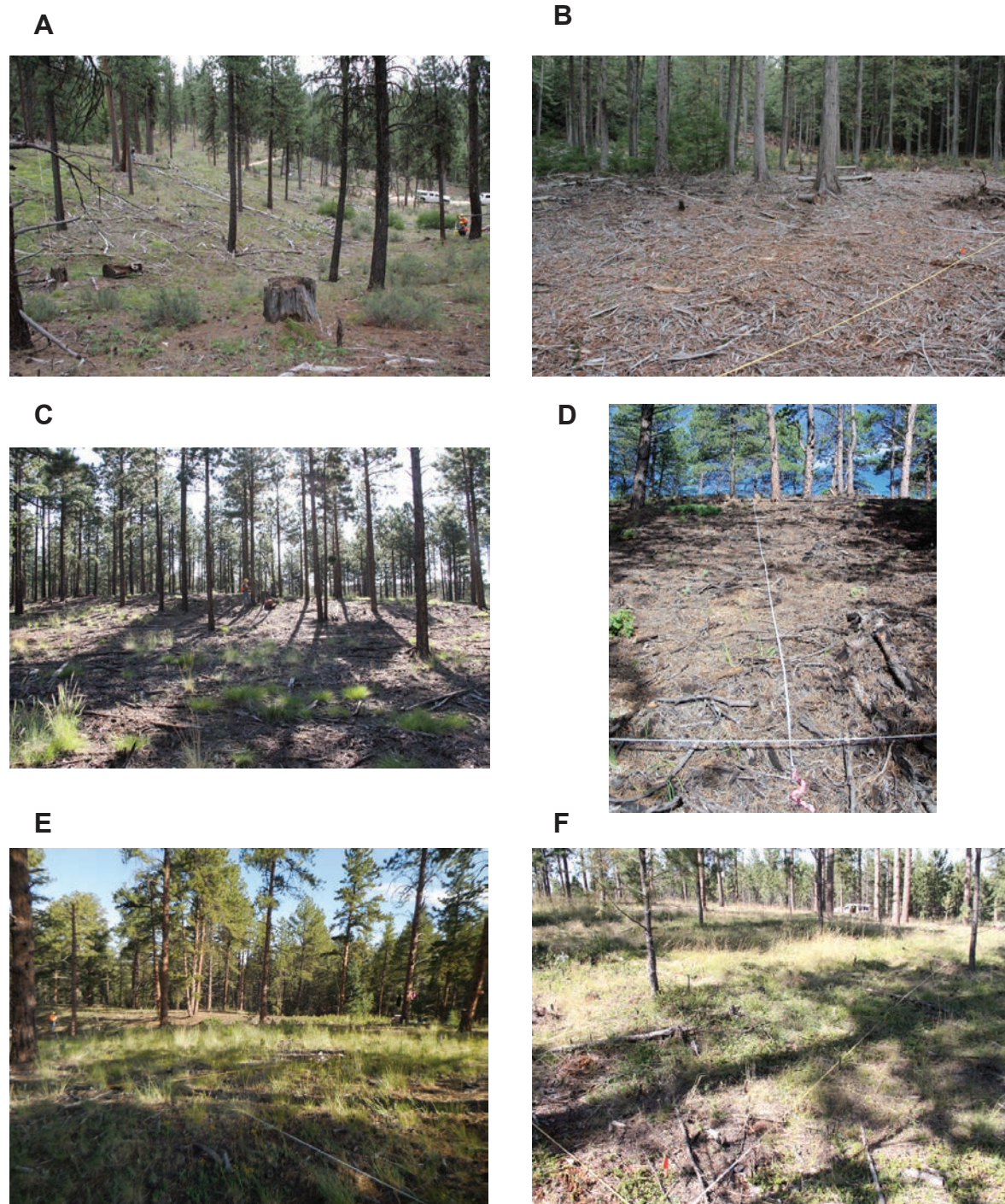
Figure 3—A representative selection of sites examined, showing the range of forest types, mastication types, and times since treatment covered by this study: (A) Amber site near Idaho City, Idaho, masticated in 2004 with rotating head, sampled in June 2014; (B) Priest River site within the Priest River Experimental Forest (site PR3), Idaho, masticated in 2011 with horizontal drum, sampled in October 2013; (C) Valles Caldera site (VC1) near Los Alamos, New Mexico, masticated 2007–2008 with horizontal drum, sampled in July 2014; (D) Skelton site within the San Juan National Forest, near Woodland Park, Colorado, masticated 2010–2011 with rotating head, sampled in July 2014; (E) Manitou Experimental Forest site (MEFChip) near Woodland Park, Colorado, masticated in 2004 by chipping, sampled in July 2014; (F) Black Hills Experimental Forest near Nemo, South Dakota (BHMow), masticated in 2012 by mowing, sampled 2014.

Figure 4—Location of the 15 study sites. Site codes are defined in table 4.
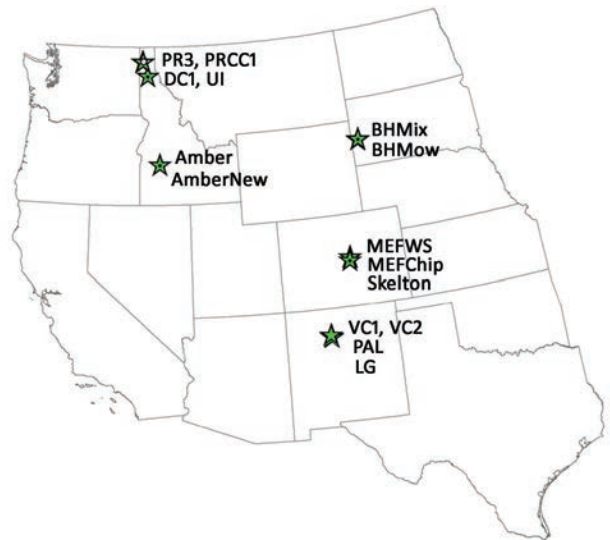
to New Mexico in the U.S. Rocky Mountains and to South Dakota in the Great Plains (fig. 4). Before treatment, all stands were dense, pole-size or mature stands with high fire hazard. We also had four treated areas in northern Idaho that represented more mesic sites with higher rainfall and cooler conditions. In this study we refer to the "climate" factor (CLIMATE) to describe differences in the two types of sites based on annual rainfall; the 11 "dry" sites were composed of mixed ponderosa pine forests with annual average rainfall less than 40 cm, and the four "moist" sites had annual average precipitation of over 40 cm and were composed of many other tree species including grand fir (*Abies grandis*) and western redcedar (*Thuja plicata*).

All areas were treated using four general types of mastication equipment (table 4, fig. 1). A vertical shaft cutting head with fixed teeth was used on six sites, a horizontal shaft cutting head with fixed teeth was used on another six sites, two sites were treated with a horizontal shaft with swinging knives, and one site was chipped (table 4). All sites had a history of frequent fires before European settlement; but since the early 1900s, fires had been successfully suppressed, thereby creating dense canopies and heavy surface fuel loadings. Pretreatment stand summaries were not available for many of these sites.

2.2 Field Sampling

Field sampling was conducted within a 30-m × 50-m macroplot located in an area within each study site that broadly represented the general conditions of the mastication treatment within the treatment unit. The 30-m sides of the rectangular macroplot were oriented up the slope and the 50-m sides were established perpendicular to the slope (fig. 5). We recorded the latitude and longitude at each corner of the macroplot, and at several points on a grid within the macroplot, using a global positioning system.

Within the macroplot, a duel subsampling design was employed that included both microplot and grid sampling. Most variables used to describe the masticated fuelbed were collected or sampled within 20 microplots that were established along two 30-m lengths within the macroplot using guidelines recommended by Hood and Wu (2006) (fig. 5). We measured several fuelbed properties in situ within each of the 20 microplots. We then collected all of the material within microplot boundaries to measure additional physical and
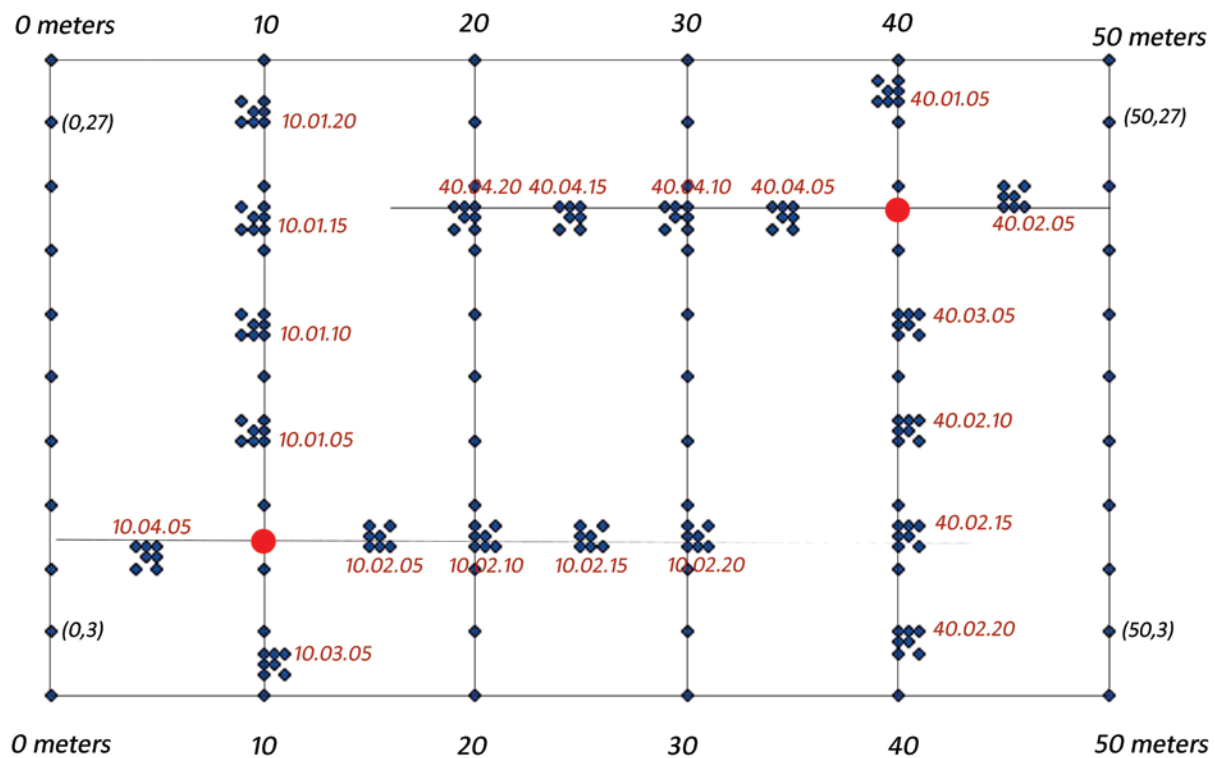
Figure 5—Grid sampling design implemented at each site. Depths of each fuelbed layer were measured at 3-m intervals along each of the six lines starting at the zero baseline. These depth plots are represented in this figure by the regularly spaced small blue diamonds within the macroplot. Small-scale sampling using Hood and Wu (2006) microplots is located at the closely spaced dots along the lines at 10 m and 40 m that form the tightly arranged squares. The randomly located starting point for each line of microplots is designated with a large red circle.

chemical characteristics of the fuel particles, layer, and fuelbed in the lab, and to use in other phases of the MASTIDON project, including the burning, smoldering, and drying experiments.

We also sampled depths of five masticated fuelbed layers at 66 grid points within the macroplot to determine the spatial variation in fuelbed depth across the entire macroplot (fig. 5). It was impossible to establish enough microplots to accurately describe spatial properties, so we augmented the microplot data with this grid sampling. The grid and microplot depth measurements were used to compute spatial statistics that describe the spatial distribution of loading in the masticated fuelbed layers across the macroplot (Keane et al. 2012b).

2.2.1 Grid-Point Sampling

The grid-point sampling consisted of taking depth measurements using a clear plastic ruler along six 30-m transect lines. These lines were established parallel to each other at 0, 10, 20, 30, 40, and 50 m from the bottom 50-m-long boundary of the macroplot (fig. 5). Along each line, starting at zero, masticated fuelbed depths were measured every 3 m to the nearest 0.5 cm (fig. 5) for the following layers (see table 2 and fig. 7):

1. Fresh litter: Litter (leaves, fallen branches, needle accumulation, cones, seeds) that has fallen since the treatment.

2. Masticated: All masticated fuels below the new litter layer and above the duff layer.

3. Masticated-Duff: Any layer where duff and masticated fuels were mixed; this mixing occurred in many plots where machinery had churned masticated fuels into the duff layer.

4. Duff: Intact, decomposed material below the masticated layer and above mineral soil.

5. Duff-Soil: A layer where machinery mixed the mineral soil with the duff; again, a common occurrence.

These five layers were not always present at each grid point. Many plots were missing the masticated-duff layer or duff-soil layer because the masticator wheels missed the grid point and did not churn the soil. Some points did not have the masticated layer because the masticator did not deposit fuels at that particular point. Each line had 11 depth measurements for a total of 66 grid point depths. No collections of materials were taken from the grid points; therefore, there are no individual fuel loadings for these points.

2.2.2 Microplot Sampling

Once grid sampling was completed, we established 20 microplots on the 10- and 40-m transects according to the Hood and Wu (2006) methods for sampling masticated materials. A random number between 6 and 24 was chosen to delineate a starting point in meters along the 10-m line and the reverse starting point (30 minus the random number) along the 40-m line. Each of these random points marked the intersection of four transects running in the four cardinal directions (fig. 5). Microplots were 1 m × 1 m and established 5 meters from this cross point. The microplots were oriented as shown in figure 5, where, facing uphill, the bottom left corner was placed at the appropriate meter mark. A photograph was taken of the microplot from below its downhill side. Finally, we established a 0.25-m^2 (0.5-m × 0.5-m) quadrat at the lower left corner of each microplot from the downhill side. A photograph of the quadrat was also taken.

Depths of the five masticated fuelbed layers were measured at the corners of the microplot and at the corners of the quadrat using the same techniques as those described for the grid sampling. These depths were used to add smaller scales of sampling to the grid points for spatial analysis and to compute bulk densities in the lab analyses (section 2.4.2). After all depth measurements were taken, all materials within the quadrat were collected down to the mineral soil, then sorted into three layers (fresh litter, masticated fuels, duff) and placed in paper bags that were labeled as to site, transect, location along transect segment, date, photo number, and fuelbed category. We could not sort the material into the same five layers used in the grid point and microplot depth measurements because it was too difficult to separate these categories in the field during the destructive sampling. As a result, we collapsed the masticated-duff, duff, and duff-soil layers into just one bag and called it duff. The duff bag was sorted in the laboratory into its proper components. We did not collect live biomass from shrubs, herbs, or logs because they were rare and beyond the scope of this study. Logs were present within the microplots, but they were not measured in the MASTIDON project because of their rarity. The collections from the University of Idaho sites (UI, table 4), used in collaboration with this study, were done with slightly different methodologies and these are documented in Lyon (2015).

2.3 Laboratory Tasks

Lab tasks consisted of the following five broad types of activities: (1) sorting fuel particles, (2) measuring and weighing a subsample of individual particles, (3) obtaining particle densities from subsamples, (4) analyzing fuels to estimate heat content, lignin, and cellulose + hemicellulose fractions from subsamples, and (5) conducting chemical analysis on particles from subsamples for carbon and nitrogen concentrations. We randomly selected 10 of the 20 microplot collections to process for lab measurements (table 3). Material from the other 10 microplots was used in other phases of the MASTIDON project not presented in this report. A total of 151 microplots were processed.

2.3.1 Sorting

The first step in the processing of a masticated sample for physical description was to sort collected material into the major components of the masticated fuelbed (fig. 2). Fresh litter was processed just as it was collected in the field without sorting or sizing. Masticated wood and bark were sorted into 15 shape categories according to the criteria in table 5, and into three size categories (1-, 10-, 100-hr fuels) (fig. 6). The duff collected in the field was cleaned of all fresh litter, bark, and wood particles that belonged in the other categories. The only remaining materials in the duff bag were pieces of debris less than 6 mm (0.25 inch).
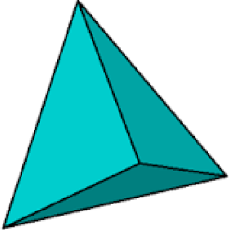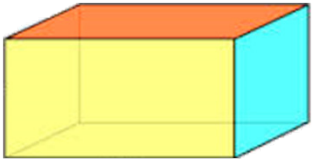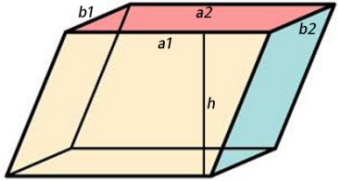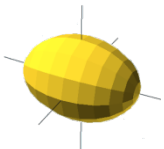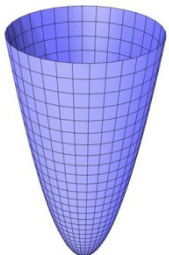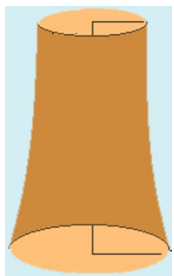
2.3.2 Physical Measurements

After sorting the particles collected from each quadrat sample, we oven-dried the particles at 90 ºC for 2 days and then weighed them to compute total load in each shape, size, and layer class. We then randomly selected a subset of particles from each shape and size class to measure their individual dimensions and obtain their particle dry weight (PW). We tried to select at least 5 percent of the total number of particles for the subsample to conduct the finer scale measurements and weights on individual particles. However, in many cases, there were fewer than 10 particles available, so we could select only 1 or 2 particles for the subsample. In some cases, there were more than 200 particles, such as 1-hr parallelograms (table 5), so we selected a maximum of 10 particles for the subsample. For the fresh litter, bark pieces, wood chips, and duff, a standard 20 percent of the field bag by total bag weight (not individual material pieces) was measured to create the subsample for weight and moisture content measurements. Length (mm), width (mm), and height (mm) were measured on each woody particle to the nearest 0.1 mm using a caliper connected to a computer to capture measurements. Other dimensional measurements were taken for each particle depending on the shape because we needed to compute volume and surface area for each particle (table 5).

A second subsample included a random collection of particles of four shape types—cylinder (circular cross-section), pyramid (triangular cross-section), parallelepiped (multi-sided polygon cross-section), and wood chips—and the three size-class categories on which to conduct chemical analyses (table 5). These shapes were selected because most particles were classified into these four shapes. A third subsample was taken from the duff component only. Small samples of duff were placed in a crucible for drying. This subsample was used to determine mineral content at the microplot.

After being measured, each subsample was weighed as a group and individually. Wet weights were taken for the 20-percent subsamples of duff, fresh litter, wood chips, and

Table 5—Description and illustration of the 13 shapes chosen to estimate volume and surface area of masticated woody particles.

Shape	Description	Diagram
Cylinder	3D circular polygon, usually with varying widths along length. Represented by complete branches >6.5 mm long. Circular cross section	
Pyramid	3D polyhedron with four faces and three prominent sides; angles off each vertex vary. Triangular cross-section.	
Rectangular parallelepiped	3D polyhedron with six faces and four prominent sides; adjacent sides of unequal length; angles close to 90º at each vertex. Rectangular cross-section.	
Parallelepiped	3D polyhedron with six faces; faces are parallelograms lying in pairs of parallel planes; four prominent sides, angles not 90º at each vertex. Varying lengths of sides can result in equilateral, trapezoidal, rhomboidal, kite-like, or trapezium sub-shapes.	
Ellipsoid	3D polygon with plane surfaces that are all ellipses or circles, no faces, no distinct sides; ends tapered; egg shaped. Elliptical cross-section.	
Elliptic paraboloid	Quadratic surface shaped like cup or bowl; no faces; edge surface curved to ground with no outward flares at base.	
Neiloid frustrum	Quadratic surface shaped like the lower portion of a tree trunk; no straight faces, edge surface curved to ground with outward flares; top usually shaped as in elliptic paraboloid (above) but lower edge flares like tree trunk base.	

Shape	Description	Diagram
Semi-cylinder	3D polygon with no faces; two sides (one curved, one flat); one-half of a cylinder.	
Wood chip	Thin, small pieces of wood greater than 6.5 mm long but less than 3.0 mm thick; classifies as 1-hour size class.	
Wood ribbon	Pieces of wood greater than 6.5 mm long, very flexible, and various widths; flexible enough to twist and turn without breaking.	
Bark ribbon	Pieces of bark greater than 6.5 mm long, very flexible, and various widths; similar to wood ribbon, it is flexible enough to twist and turn without breaking.	
Bark piece	Pieces of bark greater than 6.5 mm but less than 25 mm at longest point; inflexible; 1-hour and 10-hour size classes combined.	
Bark chunk	Pieces of bark greater than 25 mm but less than 75 mm at longest point. Thickness varies. 100-hour size class.	

bark pieces. Although these wet weights did not represent true moisture content in the field, which was altered by drying in the paper bags while in shipping and storage, the wet weights at the time of sorting were used to eventually determine moisture content of each size class when the materials were experimentally burned. After all microplot samples were measured and weighed, they were oven-dried for more than 72 hr at 90 ºC to provide a dry weight for the fuel type and dry weight for each individual particle. All dried subsamples and particles were then used in the following physical and chemical analyses.

Figure 6—Masticated fuel particles from one sample bag, sorted by shape (table 5) and size: (a) masticated fuel shapes and (b) other fuel shapes.

2.3.2.1 Particle Density

The particle densities (PDs) were estimated using a two-fluid displacement process that has historically been used to determine density in soils or duff (Williamson and Wiemann 2010). The method consisted of slowly submerging particles in a large cylindrical tube containing a combination of two fluids (fig. 7). The upper fluid was 100 percent kerosene; the lower fluid was a solution of 50 percent glycerin and 50 percent water. Both fluids were approximately 20 cm deep to allow enough room for submersion of large particles; the cylinder sat on a lift so that it could be raised and lowered as needed during the submersion process. The particle was attached to plastic line that had a large lead weight at the end to keep it submerged. The line with the lead weight and the particle was attached to a scale. The lead weight and line were tared by submerging them in each fluid without a particle attached and recording a weight in each fluid from the scale. Densities for each fluid were taken from the literature for inputs in the formulas that follow.

In the displacement method, the balance was first tared to zero with the particle, line, and lead weight all connected but outside of the fluids. Then the particle was slowly lowered into the kerosene until it was about 1 cm above the kerosene-glycerin boundary, and it was left at that depth for 3 minutes (fig. 7). After 3 minutes, the weight on the balance was recorded. The particle was then lowered into the glycerin-water layer to within 1.25 cm of the boundary between the two fluids and left to equilibrate and displace glycerin. After 3 minutes, the weight of the particle in the glycerin-water layer was recorded.

The PD was computed using the following equation (Sarli et al. 2001):

$$PD = PW \frac{(P_k - P_{mix})}{(W_k - W_{mix})}$$

where PD is the particle density (g cm^{-3}), PW is the particle dry weight (g), P_k and P_{mix} are the densities of the kerosene and the glycerin-water mixture, respectively (g cm^{-3});
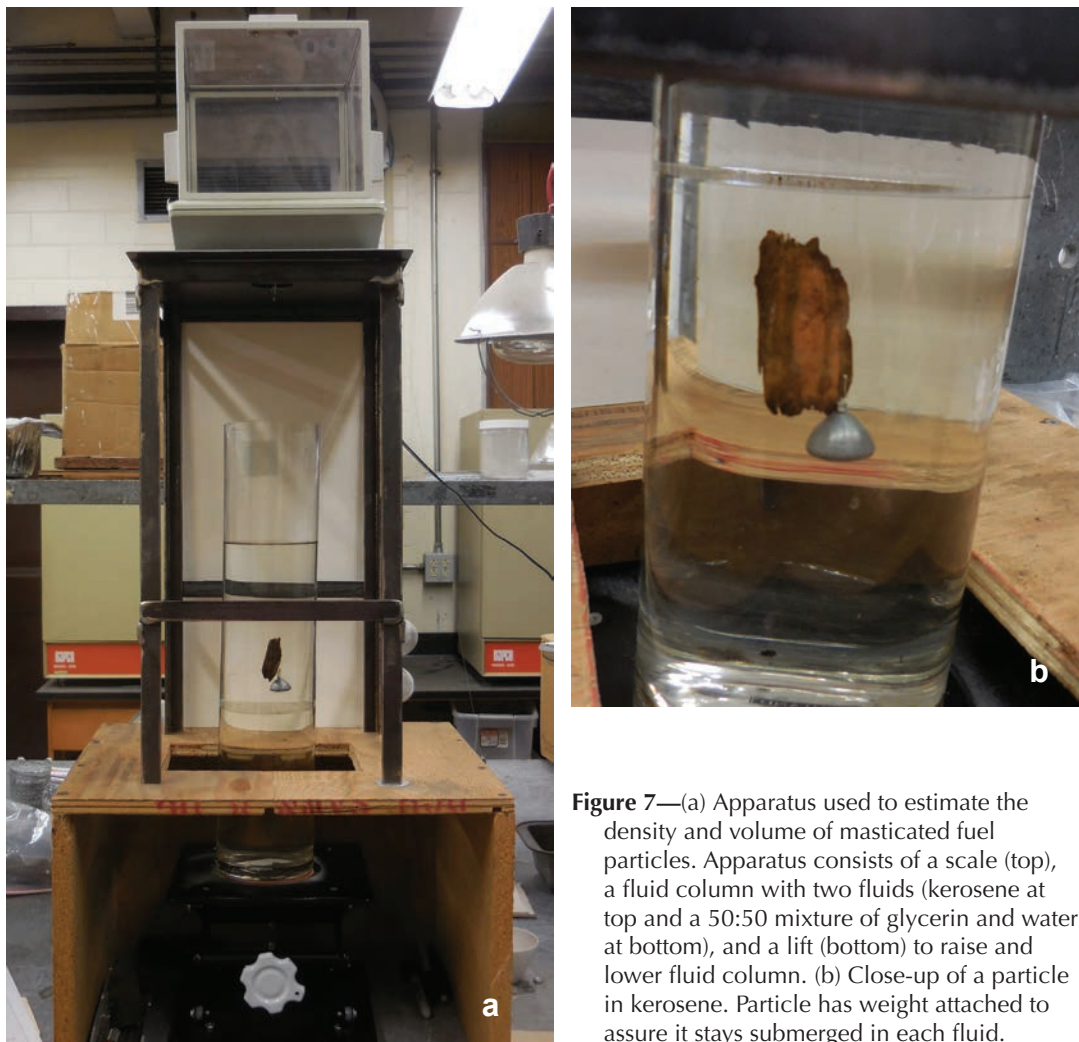
Figure 7—(a) Apparatus used to estimate the density and volume of masticated fuel particles. Apparatus consists of a scale (top), a fluid column with two fluids (kerosene at top and a 50:50 mixture of glycerin and water at bottom), and a lift (bottom) to raise and lower fluid column. (b) Close-up of a particle in kerosene. Particle has weight attached to assure it stays submerged in each fluid.

and W_k and W_{mix} are the weights (g) of the particle in the kerosene and glycerin-water mixture layers, respectively.

2.3.2.2 Surface Area

We calculated surface area (SA) by solving for particle volume (PV) from the PD measurement discussed in section 2.3.2.1 and then calculating a new length from generalized volume equations for each shape (table 4). The new length was put in generalized surface area equations.

First, PV was calculated as follows:

$$PV = \frac{PW}{PD}$$

where PV is the particle volume (cm^3), PW is the particle dry weight (g), and PD is the particle density (g cm^{-3}) as obtained in the process described in section 2.3.2.1. Using PV from the particle density, we solved for a new length using the standardized shape-volume equations taken from the literature (Math.com, n.d.); we then applied the new length to standard formulas used to compute surface area for the individual particle shapes. Although not a perfect solution, the resulting surface areas were at least semi-

adjusted for the departure from a perfect shape in a manner similar to the particle densities. The method had problems, especially in the parallelograms, where a total length was measured and a mean length was calculated for the two long sides. In this case, only the mean length was adjusted in the surface area formula. Calculating new lengths in ellipses also required some assumptions, including that the longest axis was length and the shortest axis was height.

2.3.3 Chemical Measurements

We measured the ratios of carbon to nitrogen and cellulose to lignin of the masticated fuels to represent the degree of decomposition. We did this by measuring carbon, nitrogen, lignin, and cellulose + hemicellulose (both cellulose and hemicellulose) fractions in each masticated wood particle. We measured carbon and nitrogen fractions with a machine that uses a combination of flow-through carrier gas and individual, highly selective infrared and thermal conductivity detectors, and we estimated lignin and cellulose + hemicellulose fractions from heat content.

2.3.3.1 Carbon and Nitrogen Percentages
Carbon and nitrogen contents (percent) were estimated using a TruSpec® carbon nitrogen analyzer (LECO Corp., St. Joseph, MI). The particles used for this analysis came from the second set of subsamples described in section 2.3.2. Particles from four shapes and three size classes were randomly selected from each microplot for each subsample, oven dried, prepared using a Wiley® mill (Thomas Scientific, Swedesboro, NJ), and then analyzed for carbon and nitrogen percentages in triplicate. This resulted in 892 chemical samples from all 151 microplots.

2.3.3.2 Heat Content, Lignin Fraction, and Cellulose Fraction
Lignin (percent) and cellulose + hemicellulose (percent) fractions were estimated using heat contents measured with an adiabatic calorimeter and the average heat content of cellulose + hemicellulose (18.2 MJ kg^{-1}) and lignin (24 MJ kg^{-1}). The samples were from the second set of subsamples (see sections 2.3.2 and 2.3.3.1) that were oven dried and prepared for analysis using a Wiley mill.

Estimates of lignin fractions (percent) were calculated using the measured heat content (HC) of the sample and the HCs of lignin and cellulose + hemicellulose. This calculation (using the following equation) assumes fuel HC reflects a mixture of the dominant materials present in wood: lignin and cellulose + hemicellulose.

$$HC = HC_c \,(100 - LIG) + HC_l \,(LIG)$$

where HC is the heat content of the sample (MJ kg^{-1}), HC_c is the heat content of cellulose + hemicellulose (18.2 MJ kg^{-1}), LIG is the lignin fraction (percent), and HC_l is the heat content of lignin (24 MJ kg^{-1}). The cellulose percentage was estimated as 100 — LIG.

2.3.3.3 Mineral Content
Mineral content (MC) was measured only for the duff samples. The duff bag was first shaken and mixed well to combine fine duff particles and mineral soil. Three small crucibles were then half filled with materials from the shaken duff bag. The crucibles were weighed and then placed in a drying oven for at least 72 hr at 90 ºC to drive off

any water. They were weighed again after drying and then placed in a muffle furnace at 550 ºC for 24 hr. The crucibles were weighed for the last time and the mineral content was computed as a percentage based on the ratio of the remaining weight to dry weight minus the weight of the crucible.

2.4 Calculations

2.4.1 Microplot Loadings

Layer loadings (kg m^{-2}) for the destructively sampled microplot quadrats were estimated from the measured dry weights of each layer in the quadrat and multiplied by four (conversion of the 0.25-m^2 to the 1-m^2 unit area). These loadings were then used to compute the layer bulk densities (BD, kg m^{-3}) using the average depth (n = 4) at each corner of the quadrat (see section 2.4.2). We could have also estimated layer loadings for all grid points by multiplying the average layer depths (m) by the average BD values but decided against it because it would not change the spatial distribution analysis.

We then compared reference loadings with computed loadings to evaluate if the microplot is appropriately referenced by the quadrat. This was accomplished by comparing the average depth of the quadrat with the average depth of the microplot, and our preliminary evaluation found that the two were equivalent and there was no need to compute loadings from depth because the same BD could be used for both quadrat and microplot. This comparison again used regression analysis statistics to evaluate the relationship; R^2, standard error, bias, and slope statistics were computed to evaluate the goodness of fit between the observed (quadrat average depth) and predicted (microplot average depth) values.

2.4.2 Layer Bulk Density

Depths from each of the grid points at the microplot and quadrat scales were averaged to get a thickness for computing layer bulk densities for each microplot. Layer bulk densities were computed using the techniques in Keane (2015) as:

$$BD = \frac{M}{V}$$

Fuel mass (M, kg) was computed for each microplot by adding the dry weights of all fuel components in the microplot. Layer volume (V, m^{-3}) was computed by multiplying the microplot area (1.0 m^2) by the average depth (m) of four grid points located at the corners of the quadrat within which material was extracted (see section 2.2.2). Dividing M by V resulted in BD values that described the combination of particles and air spaces within microplot layers.

As previously mentioned, five masticated fuelbed layers were measured at the grid points and within the microplots, but dry weights were obtained only for three layers (fresh litter, masticated materials, and duff). Therefore, the BD for the masticated-duff-mineral combined layers was used for all three duff layers: the masticated-duff layer, the duff layer, and the duff-mineral layer.

2.4.3 Physical and Chemical Measurements

We averaged data for physical and chemical characteristics across microplots by site to create the summary tables in this report. Some characteristics, such as carbon and nitrogen content, were measured only for the masticated fuel layer. These measurements were also summarized across microplots and among sites, but their values pertain only to the masticated fuel layer. Mineral contents were measured only on the fine material less than 3 mm in size (i.e., duff) and were summarized across microplots. We also computed the composition of size and shape classes for the 15 sites based on dry weight.

2.5 Analysis

Most physical and chemical characteristics were summarized to the microplot scale using central tendency statistics across all particles measured for that microplot. Normal distributions were checked for all datasets using Q-Q plots and normal distributions were rarely found, except for the chemical variables (table 6). Nonparametric measures were used in this study because numerous Q-Q plots showed that the fuelbed and particle data were rarely normally distributed and outliers were abundant. Kendall's

Table 6—The 25 variables summarized to the microplot scale and used in the analysis to correlate the loading, physical, and chemical properties of the masticated fuelbed to fuelbed age or time since treatment.

Variable	Description	Units
LLOAD	Fresh litter layer load	$kg\ m^{-2}$
MLOAD	Masticated layer load	$kg\ m^{-2}$
DLOAD	Duff layer load	$kg\ m^{-2}$
TLOAD	Total loading of entire masticated fuelbed	$kg\ m^{-2}$
S1LOAD	Loading in 0–6 cm diameter woody size class (1 hr)	$kg\ m^{-2}$
S10LOAD	Loading in 6–25 cm diameter woody size class (10 hr)	$kg\ m^{-2}$
S100LOAD	Loading in 25–75 cm diameter woody size class (100 hr)	$kg\ m^{-2}$
LBULK	Fresh litter layer bulk density	$kg\ m^{-3}$
MBULK	Masticated layer bulk density	$kg\ m^{-3}$
DBULK	Duff layer bulk density including duff-masticated, duff-soil	$kg\ m^{-3}$
BD	Bulk density of entire masticated fuelbed	$kg\ m^{-3}$
HC	Heat content	percent
MC	Mineral content of masticated fuel layers	percent
CELL	Cellulose + hemicellulose fraction	percent
LIG	Lignin fraction	percent
N	Nitrogen fraction	percent
C	Carbon fraction	percent
CNRATIO	Carbon:Nitrogen ratio (for masticated particles only)	ratio
LENGTH	Average length of fuel particle	cm
WIDTH	Average width or diameter of particle	cm
PW	Particle dry weight	g
PD	Particle density measured for each particle in the subsamples	$g\ cm^{-3}$
SA	Surface area	cm^2
PV	Particle volume	cm^3
SAVR	Surface area:volume ratio	cm^{-1}

Tau tests from the R statistics package (R Core Team 2015) were used for these comparisons assuming two-sided hypotheses. Kendall's Tau tests are more appropriate for analyses with small sample numbers, which was the case for some of our data. Kendall's Tau also provides more information on the strength and direction of correlation for all of the analyses than does the Spearman's test (Sokal and Rohlf 1981). All correlation results were summarized from either particle or fuelbed layer measurements in a correlation table using microplots as observations. Outliers were also distinguished for each dataset using the differences in the interquartile ranges.

2.5.1 Fuel Property Relationships

We evaluated correlations of the loading, chemical, and physical fuel properties to each other using the nonparametric correlation analysis Kendall's Tau (Boddy and Smith 2009). We first computed the correlation of the loading variables to the physical and chemical variables, and then the correlations of the chemical variables to the physical variables. This correlation analysis was conducted to determine if any of the fuel properties were related to each other and thus could influence interpretation of our other statistical analyses (multicolinearity).

2.5.2 Age Relationships

We also used Kendall's Tau correlation analysis to determine relationships of all continuous variables presented in table 6 with treatment age (0–10 years), along with graphical scattergrams and goodness-of-fit statistics. Time since mastication (AGE) was used as a proxy continuous variable for "fuelbed age." We evaluated the strength of the relationship by comparing Tau values and their statistical significance.

Correlation analysis provided a means to determine significant relationships of continuous fuel variables with age in our "substitute-space-for-time" study, but we thought that major differences in biophysical conditions (moist vs. cool, wet; CLIMATE in table 4) and mastication method (MAST) across sites could overwhelm possible detection of significant relationships with age. Therefore, we used the Friedman Analysis of Variance (ANOVA) on Ranks test, which is the nonparametric equivalent to standard ANOVA (Boddy and Smith 2009; Sokal and Rohlf 1981), to determine differences in each fuel property variable (table 6) by CLIMATE and MAST. To use the Friedman analysis, all variables were standardized so that their ranges were adjusted to a similar scale and medians were comparable. We used the probability value (pval) to evaluate if there was a significant difference between CLIMATE and MAST for each variable (pval < 0.05).

Recognizing that the Friedman analysis provides limited interpretive value because of the disparity in conditions across sites, we also performed a paired analysis at sites that had two treatments in time. For this paper, we chose three pairs of sites in our 15-site study to show the effect of pairing plots that were adjacent to each other, had been treated with the same mastication technique, and had been treated two separate times: Amber (in 2004) and AmberNew (in 2010) near Boise, Idaho; LG (2006) and PAL (2012) on the Santa Fe National Forest in New Mexico; and VC1 (2007) and VC2 (2012) in the Valles Caldera in New Mexico (table 4). Because CLIMATE and MAST were held constant, we tested differences between sites in each of the pairs to detect any changes of fuel properties with age. We used the field and lab summaries

at the microplot level as observations and compared differences between the two sites using nonparametric statistic Mann-Whitney rank sum tests (Sokal and Rohlf 1981). Although this paired analysis does not provide insight into the factors that change fuel properties, results may provide support for the hypothesis that fuel properties may indeed change over time but other factors, such as CLIMATE and MAST, are masking results.

2.5.3 Spatial Analysis

The grid point depths for masticated layers were used in an analysis of the spatial variability of masticated fuelbed depths and loadings (Keane et al. 2012b). These depths resulted in a sample size of about 200 points in each macroplot. By using the Geostatistical Analyst in ARCMap 10.2.2 (ESRI 2014), the depth measures from all macroplots (sites) were explored for normal distribution and preferred trends on the landscape. Histograms, normal Q-Q plots, and trend analysis were all used within Geostatistical Analyst to explore these features. All of the depths at each site were found to be non-normal in distribution, so the values were converted with Box-Cox transformations to be more normally distributed before they were further processed with geostatistical methods.

Four spatial models (Gaussian, exponential, spherical, and pure nugget) were tested within ArcGIS 10.2 (ESRI 2014) to determine the best model describing the spatial variation at each site (Fortin 1999). Anisotrophy was taken into account in each model run. Within the model tests, the R^2 value, the average standard error, mean square error, and root mean squared error were examined to select the model that most appropriately represented the variation. "Best models" were evaluated by (1) a mean prediction error close to zero (indicating predictions were unbiased), (2) a root-mean-square standardized error close to 1 (indicating standard errors were accurate), and (3) a root-mean-square error and average standard error as small as possible (indicating that the predictions did not deviate much from the measured values). The nugget, sill, and range for the site were quantified from the best model run. Semivariograms were also computed for all points on the grid during the kriging process. Spatial autocorrelation analysis was used within Geostatistical Analyst to fit semivariograms (fig. 8) for the spatial distribution of layer depths and canopy fuel component to determine the scale at which the fuel layers in that macroplot were best measured and described.

Figure 8—Semivariogram and its characteristics. The nugget, sill, partial sill, and range are commonly used to describe the spatial variability of an ecological characteristic. Example taken from the SAS®/STAT(R) 9.3 Users Guide (SAS Institute Inc., Cary, NC).
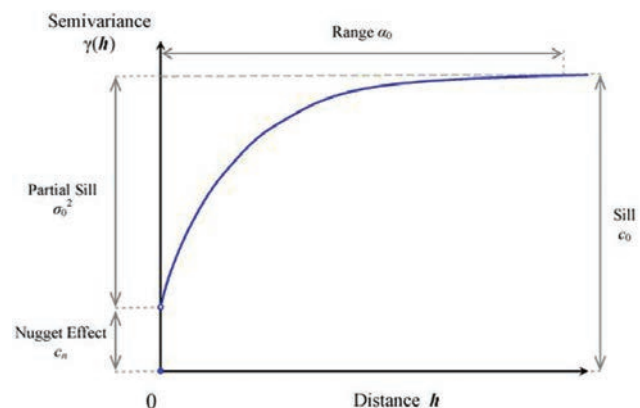
Correlations were also computed to determine if the spatial effects (range, sill, and nugget) could be related to the fuelbed age. We also evaluated whether spatial variation in the fuel variable is isotropic and whether the variation is stationary, in other words, homogeneous in space. Statistics that were used within ARCMap to describe the spatial distribution of fuel variables included a spatial autocorrelation (Moran's I) and two methods for describing clusters of material deposited during the mastication process: Cluster Outlier Analysis (also known as Anselin Local Moran's I) and Hot Spot Analysis (Getis-Ord Gi*) (ESRI 2014).

3. Results

3.1 Summary

3.1.1 Loading

Calculations from the destructively sampled microplot collections showed high total fuel loadings in all masticated fuelbeds for most sites (2.6 to 9.7 kg m^{-2}). Most of these fuels were contained in the woody masticated layer (28 to 83 percent, averaging 52 percent), compared to fresh litter and duff layers (table 7). Several sites contained high duff loadings (e.g., 4.6 kg m^{-2} on LG and 4.2 kg m^{-2} on VC1), but these sites also had the highest fuelbed loads. The duff and masticated layers had the greatest range in loading (0.6 to 4.6 kg m^{-2} and 0.8 to 4.9 kg m^{-2}, respectively). The highest total fuelbed loadings were often found in the moist, northern Idaho sites (PR3 and PRCC1, with greater than 5.0 kg m^{-2}) and the Valles Caldera sites (VC2 and VC1, with greater than 6.0 kg m^{-2}). Loading standard errors (SE) were largest in the masticated fuel layer (0.4 to 2.5 kg m^{-2}) because of the great variability in woody particle sizes, and lowest in the fresh litter layer (0.07 to 0.3 kg m^{-2}). In general, the SEs across the averaged microplots ranged from 7 to 40 percent of the mean across all layers.

The masticated fuel layer had some of the greatest depths (0.7 to 7.4 cm) and the highest bulk densities (86.7 to 239.3 kg m^{-3}), as measured across the microplots, of all fuelbed layers because the fuel particles were mostly wood (table 7). The fresh litter layer was the shallowest (0.1 to 3.2 cm), the most porous (bulk densities from 0.7 to 128.8 kg m^{-3}), and the most variable in bulk density of the layers. Bulk densities for the total masticated fuelbed (table 7) had a somewhat small range (53.0 to 102.6 kg m^{-3}), indicating some similarity across all sites. Logistical problems prevented implementation of some of our methods on the UI site (table 4), resulting in many missing values.

Depths measured from the grid points (n = 66) were quite similar to microplot depths (n = 50), but in many cases, they were shallower and had higher SEs (table 8). The two additional layers that we used for the grid sampling (mixed masticated-duff layer and the mixed mineral soil-duff layer) had shallow depths (0.0 to 3.3 cm and 0.0 to 1.5 cm, respectively), indicating that the three layers used in the microplot particle analysis may be sufficient; five layers were not necessary (fig. 2). The SEs for depth measurements were also small across many of the five layers (0 to 30 percent of the mean). Depths are a surrogate for loading because most studies calculate loading by multiplying depths by a bulk density.

3.1.2 Physical Characteristics

Each masticated particle was described by a length, width (diameter), and height. We found that, overall, most of the masticated fuel particles were long (3.5 to 9.3 cm), thin (0.9 to 1.2 cm), and short (0.5 to 0.9 cm), but with remarkable variability among the 15 sites (table 9). Some sites had large chunks of masticated materials (Amber, AmberNew, and PR3), and others had fine slivers (MEFChip, LG, and VC2), as a consequence of the silvicultural prescription parameters and mastication method. Most of the variation among masticated particle sizes across sites occurred in the length measurements, which also had the highest SEs within sites (0.05 to 0.4 cm). Width and height values were surprisingly similar with SE values that were less than 0.02 cm (<5 percent of the mean).

Table 7—Summary of the physical characteristics, and standard error (SE), of masticated fuelbeds by study site and fuelbed layer, computed from microplot samples. Note that all duff layers were combined into one in the microplot measurements due to difficulties separating the layers in the field. Sites are listed in order of time since treatment (age). Site codes are defined in table 4. NA = value not available.

Site code	Mastication age (yrs)	Number of microplots	Fresh litter Load (kg m⁻²)	SE (kg m⁻²)	Depth (cm)	SE (cm)	Bulk density (kg m⁻³)	SE (kg m⁻³)	Duff Load (kg m⁻²)	SE (kg m⁻²)	Depth (cm)	SE (cm)	Bulk density (kg m⁻³)	SE (kg m⁻³)
Amber	10	10	1.29	0.17	3.1	0.3	42.77	4.81	0.72	0.7	2.8	0.20	29.12	6.94
MEFChip	10	14	1.10	0.26	2.2	0.3	58.84	15.88	1.64	0.3	2.2	0.36	75.70	13.31
DC1	9	10	0.48	0.08	2.5	1.2	50.30	11.06	0.92	0.6	2.9	0.36	38.19	13.10
MEFWS	9	15	0.73	0.15	1.7	0.2	39.84	6.72	0.73	0.2	0.4	0.19	83.53	34.91
LG	8	9	0.72	0.13	2.2	0.2	32.91	6.10	4.56	0.5	4.5	0.72	106.70	17.54
PRCC1[a]	6	10	0.28	0.07	0.1	0.1	0.69	0.69	0.61	0.7	2.9	0.17	26.51	8.75
VC1	6	10	0.65	0.08	2.3	0.3	31.11	5.99	4.21	1.0	4.6	0.92	162.56	54.72
AmberNew	4	10	1.24	0.25	3.2	0.4	41.29	7.94	0.82	0.5	2.3	0.23	33.54	8.97
Skelton	3	10	1.63	0.27	2.0	0.3	95.12	20.83	0.76	0.3	1.5	0.35	45.09	23.94
PR3	2	10	0.60	0.11	2.5	0.9	33.87	8.55	3.71	1.3	5.6	0.87	55.39	16.13
BHMIX	2	10	1.72	0.19	1.8	0.3	128.81	38.82	1.25	0.3	3.1	0.19	43.30	6.08
BHMOW	2	10	1.07	0.18	1.6	0.2	86.22	20.36	0.68	0.4	2.2	0.16	36.58	8.63
PAL	2	10	0.68	0.16	1.2	0.3	120.30	54.53	3.28	0.6	3.6	0.31	129.86	33.03
VC2	2	10	0.97	0.21	2.5	0.6	48.07	14.53	1.62	0.5	2.3	0.29	128.67	44.68
UI[b]	0	3	1.15	0.27	NA	NA	0.00	0.00	0.56	NA	NA	0.12	0.00	0.00

Site code	Mastication age (yrs)	Number of microplots	Masticated Load (kg m⁻²)	SE (kg m⁻²)	Depth (cm)	SE (cm)	Bulk density (kg m⁻³)	SE (kg m⁻³)	Total fuelbed Load (kg m⁻²)	SE (kg m⁻²)	Depth (cm)	SE (cm)	Bulk density (kg m⁻³)	SE (kg m⁻³)
Amber	10	10	1.93	0.41	1.7	0.4	157.50	69.50	3.94	1.0	7.6	0.75	52.96	6.98
MEFChip	10	14	2.23	0.38	1.8	0.4	171.41	49.21	4.97	0.7	6.2	0.82	77.30	6.00
DC1	9	10	4.55	1.18	4.4	0.8	140.36	44.42	5.95	1.7	9.8	1.39	64.86	12.80
MEFWS	9	15	1.52	0.43	1.4	0.5	86.66	17.27	2.98	0.6	3.6	0.64	90.95	12.70
LG	8	9	3.39	0.67	2.0	0.4	239.29	67.15	8.67	0.7	8.7	1.17	102.60	13.16
PRCC1	6	10	4.29	0.99	7.4	2.1	102.25	37.52	5.18	2.5	10.5	1.13	72.49	24.12
VC1	6	10	4.85	0.77	3.3	0.6	214.50	73.90	9.71	1.1	10.2	1.42	93.85	6.93
AmberNew	4	10	2.63	0.61	3.1	0.7	89.50	9.08	4.69	1.0	8.5	0.84	52.30	5.49
Skelton	3	10	2.06	0.45	2.6	0.8	137.30	53.02	4.45	0.9	6.0	0.71	79.39	13.95
PR3	2	10	3.27	0.82	3.6	1.5	140.39	70.32	7.58	1.6	11.7	1.23	70.53	12.81
BHMIX	2	10	1.17	0.24	0.7	0.2	147.10	41.95	4.13	0.5	5.6	0.48	75.34	7.32
BHMOW	2	10	0.82	0.18	1.0	0.3	123.38	38.10	2.57	0.7	4.7	0.19	65.70	8.49
PAL	2	10	3.55	0.80	2.7	0.9	177.93	44.19	7.51	0.9	7.5	1.07	101.55	10.72
VC2	2	10	3.85	0.90	2.9	0.9	155.06	46.32	6.44	1.5	7.6	0.98	90.40	10.26
UI	0	3	4.56	2.47	NA	NA	0.00	0.00	6.27	NA	NA	2.48	0.00	0.00

[a] Depths of fresh litter in 9 of the 10 microplots for PRCC1 are zero, which results in zero values for the bulk densities in those microplots.

[b] Depths for the UI plots were taken by the University of Idaho and not provided for the three plots furnished to this study.

Table 8—Summary of the grid-point depths, and standard error (SE), for each fuelbed layer by study site. The depths of the mixed masticated-duff and mixed soil-duff are considered portions of the duff layer depth because the three layers could not be separated in the laboratory. Sites are listed in order of time since treatment (age). Site codes are defined in table 4.

Site code	Mastication age (yrs)	Fresh litter		Masticated		Mixed masticated-duff		Duff		Mixed soil-duff		Total depth (cm)	
		Avg. depth[a] (cm)	SE (cm)	Avg. depth (cm)	SE (cm)	Avg. depth (cm)	SE (cm)	Avg. depth (cm)	SE (cm)	Avg. depth (cm)	SE (cm)	Avg. depth (cm)	SE (cm)
Amber	10	3.2	0.2	3.4	0.3	0.4	0.1	3.1	0.2	0.2	0.1	10.3	0.5
MEFChip	10	2.3	0.1	2.2	0.2	0.0	0.0	2.5	0.2	0.0	0.0	7.0	0.3
DC1	9	2.4	0.3	4.2	0.4	0.1	0.0	2.3	0.2	1.5	0.2	10.4	0.6
MEFWS	9	2.0	0.1	1.3	0.1	0.0	0.0	0.7	0.1	0.0	0.0	3.9	0.2
LG	8	2.1	0.1	2.9	0.2	3.1	0.3	2.3	0.2	0.3	0.1	10.7	0.3
PRCC1	6	0.1	0.0	7.7	0.7	0.4	0.1	3.4	0.3	0.1	0.1	11.8	0.8
VC1	6	2.1	0.1	3.4	0.3	3.3	0.4	1.3	0.2	0.0	0.0	10.1	0.4
AmberNew	4	3.4	0.2	3.9	0.3	0.5	0.1	3.7	0.3	0.6	0.1	12.2	0.6
Skelton	3	2.9	0.2	2.5	0.2	0.3	0.1	2.1	0.2	0.0	0.0	7.8	0.4
PR3	2	3.6	0.4	3.1	0.4	1.7	0.3	3.3	0.3	0.7	0.2	12.4	0.6
BHMix	2	1.7	0.1	1.3	0.1	0.2	0.1	2.7	0.1	0.0	0.0	5.8	0.2
BHMow	2	1.8	0.1	1.4	0.1	0.3	0.1	2.6	0.2	0.1	0.1	6.2	0.3
PAL	2	1.5	0.1	2.2	0.2	1.4	0.2	2.3	0.2	0.1	0.1	7.5	0.3
VC2	2	2.2	0.1	2.8	0.2	1.3	0.2	1.7	0.2	0.1	0.0	8.1	0.4

[a] Depths were taken at grid points every 3 m along transects spaced 10 m apart (see fig. 5). Points totaled 66 per macroplot. No microplot depths were included in this summary.

Table 9—Summary of the physical characteristics, and standard error (SE), of the masticated particles, by site for the masticated fuel layer only. For each characteristic, the mean value was calculated using all particles found at the site no matter what their shape; n = number of particles across all 10 microplots at the site. Sites are listed in order of time since treatment (age). Site codes are defined in table 4.

Site code	Mastication age (yrs)	n	Particle length LENGTH (cm)		Particle width-dia WIDTH (cm)		Particle height PH (cm)		Particle dry weight PW (g)		Particle density PD (g cm^{-3})		Particle surface area SA (cm^2)		Particle volume PV (cm^3)		Surface area: volume (SAVR) (cm^{-1})	
			Mean	SE	Mean	SE	Mean	SE	Mean	SE	Mean	SE	Mean	SE	Mean	SE	Mean	SE
Amber	10	257	8.91	0.14	1.24	0.02	0.77	0.01	5.50	0.89	0.40	<0.01	116.93	6.46	15.39	2.60	25.40	1.08
MEFChip	10	425	3.49	0.05	1.05	0.01	0.64	0.01	1.77	0.40	0.36	<0.01	19.03	0.52	11.48	2.31	17.47	0.28
DC1	9	621	5.98	0.08	1.05	0.01	0.68	0.01	4.48	0.97	0.37	<0.01	56.31	2.53	3.80	0.78	19.57	0.38
MEFWS	9	321	5.38	0.11	1.15	0.01	0.79	0.01	4.92	1.21	0.41	<0.01	40.63	1.81	12.00	2.99	18.90	0.55
LG	8	320	4.91	0.10	1.14	0.02	0.76	0.02	3.96	1.43	0.35	<0.01	35.34	1.46	11.75	4.29	15.76	0.49
PRCC1	6	325	7.27	0.15	1.16	0.03	0.69	0.01	7.68	2.75	0.36	<0.01	70.55	4.30	21.41	8.68	20.23	0.62
VC1	6	431	5.20	0.06	1.22	0.02	0.77	0.01	3.34	0.45	0.38	<0.01	43.31	1.71	7.81	1.14	17.07	0.57
AmberNew	4	342	9.25	0.16	1.13	0.02	0.71	0.01	6.76	1.13	0.46	<0.01	85.78	3.51	16.58	2.91	29.21	1.09
Skelton	3	364	7.82	0.13	1.17	0.02	0.79	0.01	5.26	0.87	0.47	<0.01	69.31	3.24	3.98	0.46	20.44	0.60
PR3	2	923	8.11	0.09	0.94	0.01	0.49	0.01	2.44	0.26	0.41	<0.01	28.61	0.65	11.64	2.03	21.18	0.38
BHMix	2	251	6.50	0.12	0.94	0.02	0.58	0.01	2.81	0.68	0.38	<0.01	44.68	1.60	7.54	2.27	24.75	0.78
BHMow	2	207	5.23	0.10	0.92	0.02	0.53	0.01	2.00	0.56	0.41	<0.01	36.34	1.49	5.18	1.73	23.60	0.79
PAL	2	325	6.50	0.10	1.30	0.02	0.79	0.01	4.55	0.67	0.40	<0.01	66.31	2.97	11.84	1.85	21.21	0.68
VC2	2	408	4.43	0.09	1.06	0.02	0.68	0.01	5.16	2.01	0.38	<0.01	38.34	1.83	12.59	5.40	18.80	0.41
UI	0	89	7.92	0.42	1.50	0.07	0.86	0.05	4.86	1.19	0.49	0.01	55.50	6.16	10.75	2.78	19.81	3.26

These three dimensions (length, width, height) were used to estimate surface area and volume, which were then used to estimate the surface-area-to-volume ratio (SAVR; section 2.3.2.2). In general, we found the SAVR values were rather similar across all sites (17.1 to 29.2 m^{-1}) with low SEs (<10 percent of the mean), even though the surface area and volume values varied greatly across sites (28.6 to 116.9 cm^2 and 3.8 to 21.4 cm^3, respectively) (table 9). Volume had higher SEs (15 percent of the mean) than did surface area (<10 percent of the mean), probably reflecting differences in estimation methods (see section 2.3.2).

An important fuel measurement in fire management is particle density (PD), which is calculated by dividing weight (PW) by volume (PV) (section 2.3.2.1). Dry weights of individual particles varied widely (1.8 to 7.7 g), with some of the highest SEs among fuel particle physical properties (>20 percent of the mean) (table 9). Yet particle densities across sites were remarkably similar (0.4 to 0.5 g cm^{-3}) with extremely low SEs (<0.01 g cm^{-3}). The heaviest particles (≥5.5 g) were on the PRCC1, AmberNew, and Amber sites, while the lightest particles (<2.5 g) were on the PR3, BHMow, and MEFChip sites. These results most likely reflect the thinning prescription and mastication machinery employed. The densest fuel particles (>0.45 g cm^{-3}) mostly occurred on the ponderosa pine sites (UI, AmberNew, and Skelton), and the least dense particles (<0.4 g cm^{-3}) were often found on a dry New Mexico site (VC1) and moist, northern Idaho site (PRCC1), probably reflecting rot in some of the particles.

Shapes of masticated particles did not vary across sites as much as we anticipated (table 10). Of the 10 wood particle shapes recognized in this project (table 5), the bulk of masticated woody fuel particles by loading (>70 percent) were mostly cylinders (6.7 to 38.6 percent) and parallelograms (4.6 to 23.7 percent), with minor amounts in semicylinder (1.6 to 10.6 percent) and pyramids (1.0 to 8.8 percent), across most sites (fig. 9). Bark particles were approximately 5 to 10 percent of the fuelbed load with most of that in fine bark pieces. Tiny duff particles made up nearly half of the loading for many of the sites (table 10), and litter accounted for another 5.5 to 41.7 percent. Some shapes, such as neiloid, wood ribbon, rectangle parallelpiped, and bark ribbon, had such low occurrences (<1 percent) that we probably could have eliminated them from the study. Most sites have representatives of every shape class in their subsamples, but the distribution of dry weight by shapes varied considerably from site to site (table 10).

More than 80 percent of the masticated fuel particles were 10-hr and 100-hr fuels (between 6 and 75 mm in width) (table 11). Nine of the 15 sites had more 10-hr fuels than 100-hr fuels. Five sites (UI, PRCC1, Amber, Skelton, and VC2) had less than 10 percent of loading in 1-hr fuels, while only three sites (MEFChip, PR3, and VC1) had more than 20 percent of loading in 1-hr particles. Three sites (PRCC1, MEFWS, and DC1) had over 55 percent of loading in 100-hr fuels, while another three sites (BJMix, BHMow, and MEFChip) had less than 30 percent in 100-hr fuels. This variation was most likely related to the machinery used, the material that was masticated, and the silvicultural prescription, which was designed to leave small-mammal habitat.

3.1.3 Chemical Characteristics

Nitrogen (N) contents varied greatly (0.4 to 0.7 percent) among masticated woody fuel particles across all the sites, but the carbon (C) proportions differed only slightly (47.6 to 51.0 percent) (table 12). The lowest N contents were on the PR3 and UI sites, in

Table 10—Percentage of loading (dry weight) of masticated fuelbed by shape (table 5) of masticated woody particle, bark, duff, and litter at each site. Percentages are based on total weight in each shape category (n = number of microplots). Sites are listed in order of time since treatment (age). Site codes are defined in table 4.

Site code	Mastication age (yrs)	n	Mean fuel load[a] (kg m^{-2})	Cylinder (%)	Ellip-soid (%)	Neiloid (%)	Parabo-loid (%)	Parallel-epiped (%)	Rectangle parallel-epiped (%)	Semi-cylinder (%)	Pyramid (%)	Wood chips (%)	Wood ribbons (%)
Amber	10	10	3.94	16.75	0.13	0.23	2.19	11.02	0.06	3.73	0.99	1.63	0.00
MEFChip	10	14	4.97	6.72	0.74	0.22	0.35	15.00	1.98	2.61	1.09	6.10	0.00
DC1	9	10	5.95	15.99	6.63	0.22	1.16	23.71	4.05	4.63	8.78	5.88	0.01
MEFWS	9	15	2.98	20.94	0.97	0.19	1.38	11.96	0.17	2.38	3.94	2.07	0.02
LG	8	9	8.67	8.83	1.71	0.24	0.49	9.27	0.20	3.39	2.94	4.17	0.00
PRCC1	6	10	5.18	38.61	5.09	0.65	6.01	18.26	0.54	2.40	5.98	2.64	0.09
VC1	6	10	9.71	6.94	5.01	0.39	1.61	13.04	0.04	1.60	3.15	5.20	0.05
AmberNew	4	10	4.69	18.81	0.32	0.16	1.92	13.63	0.02	5.76	1.08	2.10	0.00
Skelton	3	10	4.45	14.35	0.15	0.58	3.56	15.96	0.00	2.01	3.77	0.90	0.12
PR3	2	10	7.58	19.16	0.58	0.05	0.27	5.27	1.69	2.62	1.90	4.37	0.53
BHMix	2	10	4.13	11.58	0.27	0.04	0.56	6.64	0.08	2.47	0.58	1.68	0.00
BHMow	2	10	2.57	19.01	0.01	0.14	0.06	4.63	0.01	1.95	0.49	1.19	0.00
PAL	2	10	7.51	9.32	0.88	0.05	0.52	12.08	0.07	5.92	3.10	2.95	0.00
VC2	2	10	6.44	27.68	0.02	0.20	0.71	11.25	0.08	4.37	2.64	2.27	0.00
UI	0	3	6.27	25.49	11.09	0.38	0.57	10.60	0.38	10.58	3.38	2.20	0.00

[a] Mean fuel load is an average of total load by site for all microplots. It includes woody materials, bark, litter, and duff.
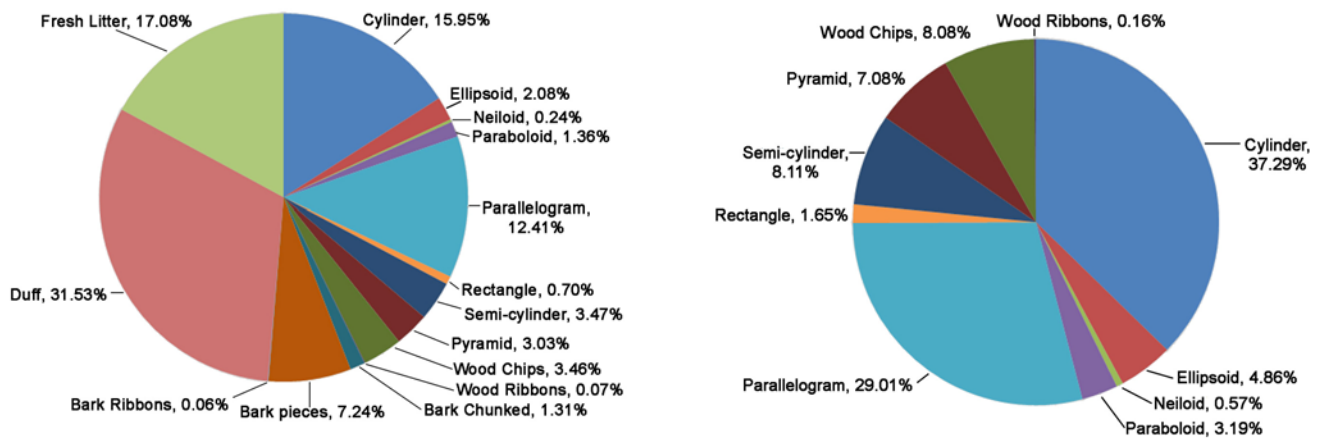
Figure 9—Shapes as a proportion of total fuelbed load across all sites for (a) woody masticated materials only, and (b) all materials constituting the total fuel load.

Table 11—Percentage of loading (dry weight) of masticated fuelbed, by size of masticated woody particles. The size classes correspond to the 1-, 10-, and 100-hr fuel moisture time lag categories used in standard fuel sampling (Keane 2015). Sites are listed in order of time since treatment (age). Site codes are defined in table 4.

Site code	Mastication age (yrs)	Number of microplots	Mean woody fuel load[a] (kg m^{-2})	1 hr (%)	10 hr (%)	100 hr (%)
Amber	10	10	1.45	7.75	41.41	50.84
MEFChip	10	14	1.73	26.35	63.13	10.52
DC1	9	10	4.23	12.16	32.67	55.17
MEFWS	9	15	1.31	10.05	33.54	56.41
LG	8	9	2.71	17.28	47.34	35.38
PRCC1	6	10	4.16	8.26	30.49	61.25
VC1	6	10	3.59	20.96	47.92	31.12
AmberNew	4	10	2.05	11.86	42.96	45.18
Skelton	3	10	1.84	7.52	49.64	42.84
PR3	2	10	2.76	24.93	42.71	32.36
BHMix	2	10	0.99	18.20	53.34	28.46
BHMow	2	10	0.71	10.94	64.31	24.75
PAL	2	10	2.62	15.28	52.29	32.43
VC2	2	10	3.17	7.16	35.42	57.42
UI	0	3	4.05	9.49	57.02	33.49

[a] Mean woody fuel load contains **only woody particles** from the masticated material. No bark is included.

Table 12—General summary of chemical characteristics by site for the masticated woody fuel layer only, except for mineral content, which is only the duff. Mean percentages by weight and the standard error (SE) are calculated across microplots (n = number of samples processed for site). All size classes and shapes within each site are combined for this analysis. Sites are listed in order of time since treatment (age). Site codes are defined in table 4.

Site	Mastication age (yrs)	n	Nitrogen N (%)		Carbon C (%)		C-N Ratio CNRATIO (dimensionless)		Duff mineral content MC (%)	
			Mean	SE	Mean	SE	Mean	SE	Mean	SE
Amber	10	62	0.54	0.02	49.66	0.22	105.65	5.62	85.82	0.39
MEFChip	10	42	0.67	0.03	48.59	0.32	79.07	3.91	88.56	0.59
DC1	9	76	0.44	0.01	51.07	0.35	127.12	4.95	84.68	0.99
MEFWS	9	43	0.62	0.03	47.60	1.20	83.30	4.21	88.96	0.96
LG	8	76	0.73	0.01	46.97	0.35	65.64	1.34	88.57	0.72
PRCC1	6	66	0.59	0.02	50.11	0.33	95.80	4.80	91.39	0.50
VC1	6	75	0.72	0.02	47.90	0.27	70.45	2.07	88.02	0.41
AmberNew	4	65	0.36	0.01	48.62	0.25	143.59	4.53	87.10	0.44
Skelton	3	64	0.48	0.02	49.58	0.31	116.38	5.53	88.00	0.47
PR3	2	58	0.35	0.02	49.27	0.23	157.66	6.65	86.15	0.41
BHMix	2	59	0.72	0.04	50.31	0.31	85.54	5.36	83.71	0.48
BHMow	2	52	0.74	0.03	50.75	0.50	75.51	4.50	85.02	0.56
PAL	2	64	0.48	0.02	47.57	0.22	110.88	4.90	85.34	0.59
VC2	2	67	0.45	0.02	49.32	0.39	120.44	4.40	90.40	0.81
UI	0	18	0.35	0.03	46.61	0.42	147.88	9.96	94.30	0.31

contrast with the BHMow, VC1, and BHMix sites, each of which had over 0.7 percent N by weight. Carbon content varied from 46.6 percent on UI to more than 51.1 percent by weight on DC1, one of the older sites. The C:N ratio (CNRATIO), perhaps the best indicator of degree of decomposition, varied from 65.6 on the LG site to more than 157.7 for PR3.

Duff mineral contents (MCs) were extremely high and somewhat consistent across all sites, ranging from 83.7 percent on the BHMix site to 94.3 percent on the UI site (table 12) with low standard errors (<0.9 percent). The highest MCs (≥90.4 percent) were found on the UI, PRCC1, and VC2 sites, while the lowest (≤84.7 percent) were found on the DC1 and BHMix sites. High MCs were a result of mastication machinery churning mineral soil into the duff. The cellulose + hemicellulose (CELL) and lignin (LIG) contents were highly variable across sites and lacked any apparent consistent patterns with age (table 13). Cellulose + hemicellulose varied from 47.3 percent at the BHMow site to 73.6 percent at the PR3 site. Lignin varied from 27.4 percent at the MEFChip site to 52.7 percent at BHMow, a newly treated unit (2 years). All CELL and LIG estimates had standard errors that were well below 5 percent except for BHMow (14.7 percent). MEFChip (10 years) had one of the highest CELL contents (72.6 percent). The heat content (HC) of masticated particles was remarkably similar across all sites and ages, ranging from 18.9 MJ kg^{-1} on the PR3 site to 20.69 MJ kg^{-1} on the BHMow site (table 13). Moreover, all of these estimates had low standard errors, ranging from 0.14 to 1.03 MJ kg^{-1} or 0.7 to 5 percent of the mean; and, similar to LIG and CELL concentrations, there was no discernable pattern across age.

Table 13—Summary of the cellulose + hemicellulose, lignin, heat content characteristics, and standard error (SE) by site for the masticated woody fuel layer only. Cells contain the mean percentage by weight and the SE of the cellulose and lignin in the masticated layer across microplots (n = number of samples processed for site). Standard errors are the same for both cellulose and lignin because of the method used to estimate values (section 2.3.3). All size classes and shapes within each site are combined for this analysis. Sites are listed in order of time since treatment (age). To convert MJ kg^{-1} to BTU lb^{-1} multiply by 430.3. Site codes are defined in table 4.

Site	Mastication age (yrs)	n	Cellulose + hemicellulose CELL (%)		Lignin LIG (%)		Heat Content HC (MJ kg^{-1})	
			Mean	SE	Mean	SE	Mean	SE
Amber	10	37	52.03	2.15	47.97	2.15	20.36	0.15
MEFChip	10	21	72.63	2.32	27.37	2.32	18.92	0.16
DC1	9	49	62.39	2.79	37.61	2.79	19.63	0.20
MEFWS	9	38	68.90	2.14	31.10	2.14	19.18	0.15
LG	8	59	60.28	2.06	39.72	2.06	19.78	0.14
PRCC1	6	31	48.62	2.88	51.38	2.88	20.60	0.20
VC1	6	32	57.57	2.94	42.43	2.94	19.97	0.21
AmberNew	4	42	61.64	2.52	38.36	2.52	19.68	0.18
Skelton	3	19	51.59	4.23	48.41	4.23	20.39	0.30
PR3	2	28	73.62	2.00	26.38	2.00	18.85	0.14
BHMix	2	22	54.65	3.60	45.68	3.84	20.20	0.27
BHMow	2	4	47.29	14.74	52.71	14.74	20.69	1.03
PAL	2	42	63.10	2.42	36.90	2.42	19.58	0.17
VC2	2	32	66.24	4.20	33.87	4.26	19.37	0.30

3.2 Spatial Variability

The semivariogram analysis of the masticated layer depths (see section 2.5.3) indicated that masticated fuelbeds have depths that vary at different scales for each site (table 14). The range is the most important statistic because it represents the inherent spatial scale of the variability of masticated loads (see section 2.5.3). We found that three sites (LG, Skelton, BHMow) had ranges smaller than 2.2 m, but most sites had ranges that varied by 3.0 to 20.0 m. Depths on two sites (MEFChip, DC1) varied by more than 32 m in range (table 14). All of these ranges had average standard errors between 1.6 and 3.5 m, resulting in high error for the lowest ranges. Most of the semivariograms had an R^2 of less than 0.5, except AmberNew ($R^2 = 0.7$) and PR3 ($R^2 = 0.5$), indicating a poor fit for most spatial models. Three model types (Gaussian, exponential, and spherical) were represented in the semivariogram analysis (table 14), indicating a wide range of curve forms and parameters across all sites.

All sites showed a nugget effect except for Skelton (nugget effect = 0) (table 14). Nugget values for mastication depth for the other sites ranged from a low of 1.7 at the PAL site to a high of 10.3 at the BHMix site. The nugget effect indicates possible measurement error in the depth measurements and represents the lowest possible semivariance that can be expected from the depth measurements. Nugget values that are comparable to the sill, such as on the MEFWS, VC1, and BHMix sites, indicate little spatial structure. Most nugget estimates were high for this study and they were remarkably variable.

Table 14—Spatial variation in depth measurements for the woody fuel masticated layer only at each site. Sites are listed in order of time since treatment (age). Site codes are defined in table 4.

Site	Mastication age (yrs)	n	Model	Nugget	Range	Sill	R^2	Avg. standard error	Mean square error	Root mean squared error
Amber	10	201	Gaussian	5.59	13.23	8.17	0.21	2.57	6.38	2.53
MEFChip	10	203	Exponential	1.90	32.29	3.87	0.31	1.58	2.55	1.60
DC1	9	199	Spherical	6.35	34.73	7.17	0.09	2.63	7.04	2.65
MEFWS	9	200	Gaussian	10.12	11.17	14.74	0.23	3.47	12.19	3.49
LG	8	203	Spherical	0.13	2.13	3.52	0.41	1.63	2.68	1.64
PRCC1	6	166	Gaussian	4.98	9.51	8.30	0.28	2.50	5.79	2.41
VC1	6	184	Gaussian	2.17	4.38	4.57	0.24	1.89	3.58	1.89
AmberNew	4	204	Exponential	1.07	4.16	6.15	0.68	2.24	5.19	2.28
Skelton	3	196	Exponential	0.00	1.54	3.43	0.35	1.82	3.63	1.90
PR3	2	212	Spherical	5.55	17.46	21.45	0.50	3.24	12.02	3.47
BHMix	2	202	Gaussian	10.27	14.50	11.92	0.13	3.42	11.18	3.34
BHMow	2	200	Spherical	3.00	1.31	7.58	0.14	2.81	7.98	2.82
PAL	2	201	Gaussian	1.70	6.98	4.56	0.35	1.60	2.99	1.73
VC2	2	189	Spherical	3.37	16.69	6.41	0.35	2.09	4.96	2.23

The sill, or maximum semivariance, also had a high range of values, from 3.4 at the Skelton site to 21.5 at the PR3 site, indicating high variation in depth values across most sites (table 14). Three sites (PR3, BHMix, and MEFWS) had sill values exceeding 10.0. The obvious trend in the depth distributions at six of the sites indicates a spatial structure.

3.3 Fuelbed Relationships

It is important to evaluate whether measured physical and chemical properties of the masticated fuelbed are correlated with each other and with other fuelbed, site, and treatment characteristics. The following sections evaluate correlations between fuel particle and fuelbed properties, and then examine whether there are any relationships between fuel properties and age, site, and treatment type.

3.3.1 Intervariable Relationships

We found few correlations among the physical and chemical properties with the seven different loading variables (table 15). The strongest correlations (Kendall's Tau >0.30), which were also statistically significant ($P < 0.05$), were the loading and bulk density for the same component: litter load (LLOAD) and litter bulk density (LBULK) (Tau = 0.51), masticated load (MLOAD) and masticated bulk density (MBULK) (Tau = 0.32), duff load (DLOAD) with duff bulk density (DBULK) (Tau = 0.52) and total fuelbed bulk density (BD) (Tau = 0.34), and total fuelbed load (TLOAD) with BD (Tau = 0.38) and MBULK (Tau = 0.33). The correlation of woody 100-hr load with fuel particle average dry weight (PW) (Tau = 0.32) and volume (PV) (Tau = 0.31) was the only other correlation above the 0.3 threshold. None of the chemical variables (HC, MC, CELL, LIG, N, C, CNRATIO) had Tau values greater than 0.2, either negative or positive (Tau = 0.20 for LLOAD to MC).

Table 15—Correlation analysis results (Kendall's Tau) for loading variables with the physical and chemical properties. Variables are defined in table 6. Number of microplots = 151; individual particles = 5,609; spatial sites = 15; carbon and nitrogen samples = 892; heat content and lignin samples = 456. Correlations are highlighted in gray if variable describes greater than 10 percent of the variation and correlation is significant at the level of $P < 0.05$.

Variable	Correlation results (Kendall's tau) with loading variables						
	LLOAD	MLOAD	DLOAD	TLOAD	S1LOAD	S10LOAD	S100LOAD
LBULK	0.51	–0.03	0.06	0.08	–0.06	0.02	0.05
MBULK	0.05	0.32	0.25	0.33	0.20	0.27	0.28
DBULK	0.03	0.17	0.52	0.34	0.14	0.11	0.15
BD	0.04	0.24	0.40	0.38	0.15	0.19	0.22
HC	0.09	0.03	–0.01	0.03	0.02	0.04	0.03
MC	–0.20	0.02	–0.08	–0.06	0.01	0.08	0.02
CELL	–0.09	–0.03	0.01	–0.03	–0.02	–0.04	–0.03
LIG	0.09	0.03	–0.01	0.03	0.02	0.04	0.03
N	0.05	–0.19	–0.00	–0.13	–0.17	–0.12	–0.16
C	0.15	–0.03	–0.13	–0.07	–0.02	–0.07	0.01
CNRATIO	–0.00	0.18	–0.00	0.13	0.16	0.11	0.16
LENGTH	0.12	0.14	–0.16	0.14	0.05	0.07	0.17
WIDTH	–0.02	0.29	0.01	0.20	0.15	0.22	0.23
PW	0.02	0.29	–0.06	0.17	0.11	0.17	0.32
PD	0.04	–0.07	–0.20	–0.11	–0.13	–0.08	–0.02
SA	0.06	0.22	–0.14	0.10	0.05	0.14	0.22
PV	0.01	0.28	–0.09	0.14	0.09	0.18	0.31
SAVR	0.07	–0.04	–0.19	–0.11	–0.11	–0.09	0.03

There were also no significant correlations of the physical properties with the chemical properties of masticated fuels (table 16). Kendall's Tau did not exceed 0.3 for any chemical variable, but the highest correlations were N and CNRATIO with PD, surface area (SA), particle length (LENGTH), particle width (WIDTH), PW, and PV (Tau ranged from 0.12 to 0.23). The surface-area-to-volume ratio and C were related to LBULK (Tau = 0.25 and 0.14, respectively).

There were no observable differences in physical and chemical particle properties across the six dominant shape categories (table 17). We could not test for statistical significance because of the small and unbalanced sample sizes across the shapes for each particle subsample. However, some major differences are worth noting. Results suggest that LENGTH, PW, and PV were larger for the cylinder than for the other shapes, and SA and SAVR were larger for the parallelepiped than for the other shapes.

3.3.2 Loading and Physical and Chemical Characteristics vs. Age

The most important result of this study was the lack of correlation of most masticated fuelbed characteristics with fuelbed age (time since treatment) (table 18; figs. 10 and 11). All correlation coefficients (Kendall's Tau) of fuelbed properties with age were less than 0.20, and most values were less than 0.10 (17 out of 25 variables). The only significant variables ($P < 0.05$) were CNRATIO, WIDTH, PV, and DLOAD, yet all of these variables

Table 16—Correlation analysis (Kendall's Tau) results for physical properties with chemical properties. Variables are defined in table 6. Individual particles = 5,609; spatial sites = 14; carbon and nitrogen samples = 892; heat content and lignin samples = 456. Correlations are highlighted in gray if variable describes greater than 10 percent of the variation and correlation is significant at the level of $P < 0.05$.

Variable	Correlation results (Kendall's Tau) with chemical variables						
	HC	MC	CELL	LIG	N	C	CNRATIO
LBULK	–0.04	–0.25	0.04	–0.04	0.04	0.14	–0.01
MBULK	0.00	–0.10	0.00	0.00	0.00	0.05	0.01
DBULK	0.02	–0.02	–0.02	–0.02	0.08	–0.12	–0.08
BD	0.01	0.02	–0.01	0.03	0.04	–0.05	–0.06
LENGTH	–0.02	–0.07	0.02	–0.02	–0.22	0.01	0.23
WIDTH	0.03	0.03	–0.03	0.03	–0.21	–0.10	0.17
PW	0.00	0.07	–0.00	0.00	–0.18	–0.01	0.17
PD	0.02	0.05	–0.02	0.02	–0.23	–0.05	0.23
SA	0.05	–0.04	–0.05	0.05	–0.22	0.00	0.21
PV	0.03	0.05	–0.03	–0.03	–0.15	–0.06	0.12
SAVR	0.00	–0.13	0.00	–0.00	–0.05	–0.07	0.07

Table 17—Summary of physical and chemical characteristics of masticated fuel particles by the four shapes with the greatest loading (table 5). Values are averages of all samples for each shape and include all size classes in the average. Number of microplots = 151; individual particles = 5,609; spatial sites = 15; carbon and nitrogen samples = 892; heat content and lignin samples = 456. Note: chemical measurements were only performed on these four shapes and they were separate samples from those analyzed for all other characteristics. Dashes represent missing values.

Variable	Cylinder	Parallelepiped	Pyramid	Wood chips
HC	19.94	19.54	19.83	19.21
MC	–	–	–	–
CELL	57.98	63.68	59.62	68.49
LIG	42.06	36.32	40.42	31.51
N	0.58	0.50	0.50	0.70
C	49.92	48.85	49.08	47.57
CNRATIO	102.93	113.83	113.11	75.92
LENGTH	103.85	48.01	53.00	–
WIDTH	8.62	12.82	9.07	–
PW	8.25	2.73	2.90	1.46
PD	0.45	0.36	0.39	0.33
SA	34.94	120.91	11.86	–
PV	17.85	6.90	7.18	–
SAVR	7.87	53.80	8.07	–

Table 18—Correlation analysis results (Kendall's Tau) for the relationship of fuelbed age (AGE) to all loading, physical, and chemical characteristics of fuelbed layer and particles for all sites and for only the ponderosa pine–dominated sites (PP sites or dry sites in table 4), and results of the Friedman Analysis of Variance (ANOVA) on Ranks testing for differences in fuel characteristics by mastication method (MAST) and site type (dry vs. moist – CLIMATE in table 4). The Friedman tests were run on standardized variables to arrange median values on the same scale. Kendall's Tau correlations are highlighted in gray when greater than 10 percent of the variation was described and correlation was significant at the level of $P < 0.05$. Probability values (pval) greater than 0.05 are highlighted in gray for the Friedman's ANOVA. Number of microplots = 151; individual particles = 5,609; spatial sites = 15; carbon and nitrogen samples = 892; heat content and lignin samples = 456.

Variable (table 6)	Correlation		Friedman's ANOVA	
	AGE (Kendall's Tau) All sites	AGE (Kendall's Tau) Only PP sites	MAST (pval)	CLIMATE (pval)
LLOAD	–0.08	–0.08	0.569	0.464
MLOAD	0.01	0.02	0.290	0.002
DLOAD	–0.12	–0.08	0.000	0.007
TLOAD	–0.08	–0.06	0.464	0.012
S1LOAD	0.01	0.07	0.002	0.935
S10LOAD	0.01	0.01	0.371	0.684
S100LOAD	–0.11	–0.17	0.008	0.200
LBULK	–0.07	–0.19	0.569	0.001
MBULK	0.06	0.01	0.088	0.001
DBULK	–0.02	–0.05	0.018	0.001
BD	–0.01	–0.06	0.684	0.028
HC	–0.03	–0.10	0.026	0.666
MC	0.08	0.15	0.445	0.932
CELL	0.03	0.10	0.005	0.923
LIG	–0.03	–0.10	0.026	0.066
N	0.10	0.04	0.607	0.230
C	–0.03	–0.12	0.864	0.493
CNRATIO	–0.13	–0.08	0.086	0.170
LENGTH	–0.07	–0.05	0.867	0.314
WIDTH	0.13	0.16	0.044	0.131
PW	0.07	0.06	0.615	0.179
PD	–0.12	–0.05	1.000	0.029
SA	0.03	–0.05	0.867	0.131
PV	0.13	0.08	0.502	0.314
SAVR	–0.12	–0.17	1.000	0.867

had Kendall's Tau less than 0.20 (table 18). We found a completely different set of notable correlations when we used only the PP sites in our correlation analysis (table 18). For the PP sites, the correlation of 100-hr fuel loading (S100LOAD), LBULK, SAVR, and WIDTH with age had Kendall's Tau values greater than 0.15.

A closer look at the relationship of physical properties to age shows high variability across microplots within the site(s) that represent a treatment age (fig. 10). Regression lines
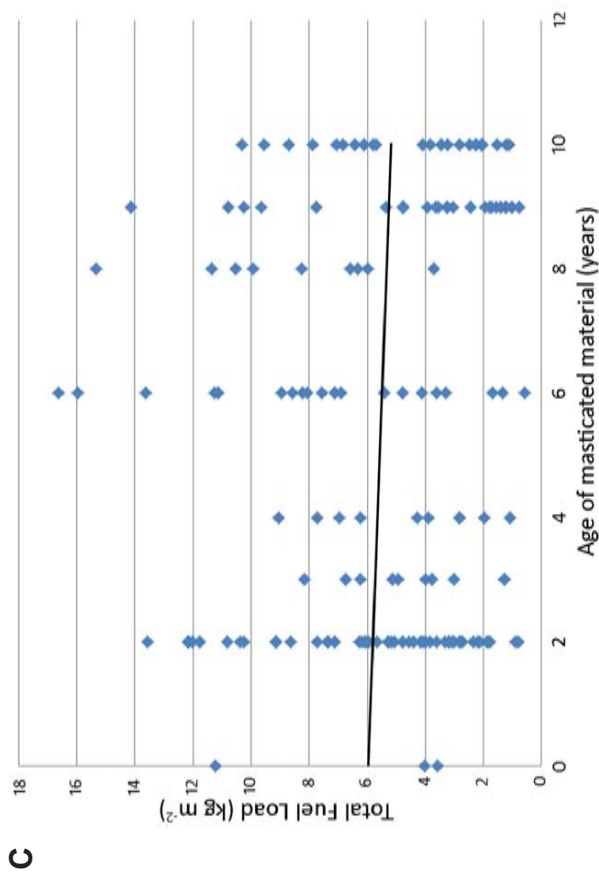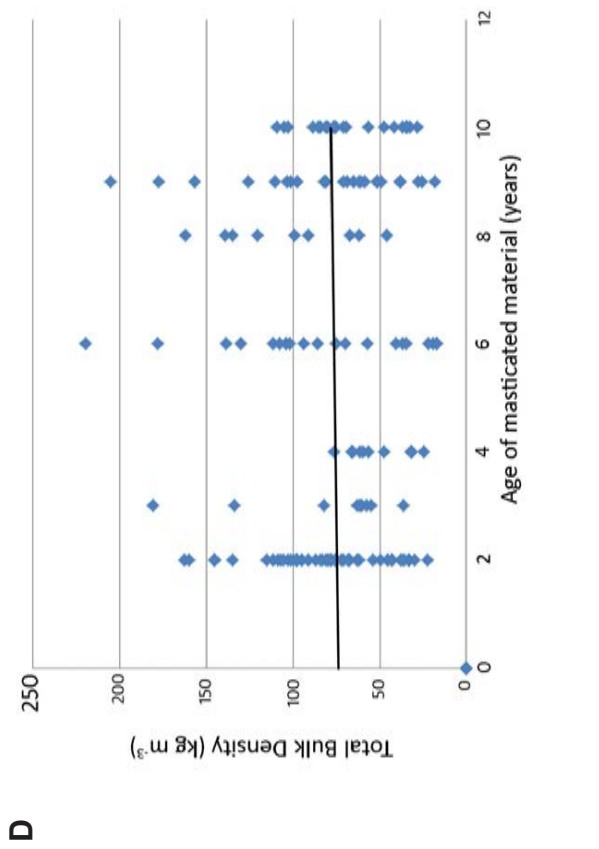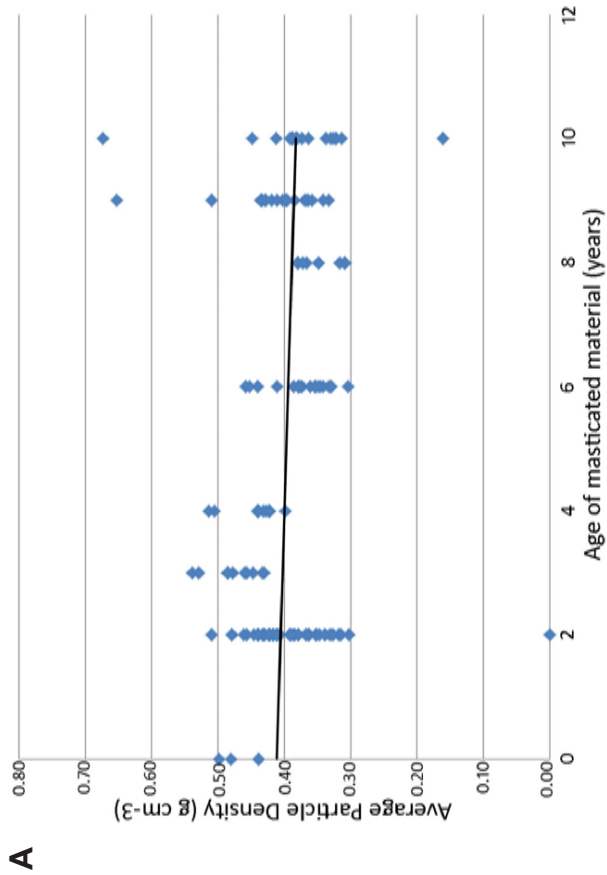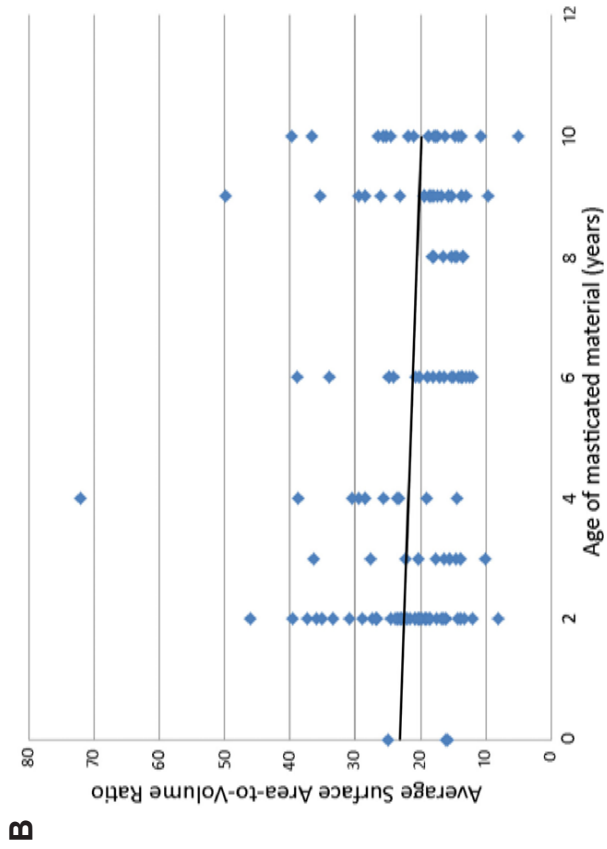
Figure 10—The four loading and physical variables with the most significant correlation with treatment age (time since treatment) and the most importance to fire behavior prediction: (a) particle density, (b) particle surface-area-to-volume ratio, (c) total fuelbed loading, and (d) total fuelbed bulk density. Linear trend lines shown. Graphs based on average values from 151 microplots.

for loading and physical variables that have the highest correlation with age (PD, SAVR, TLOAD, and BD) show slopes that are near zero with high variability about the line at any age (fig. 10). Particle density had the least variability about the regression line while TLOAD had the most. As is evident from the scattergraphs, the high variabilities of the physical fuel properties across sites appear to overwhelm all trends across time since treatment; TLOAD (fig. 10c), for example, has a range that is greater than twice the mean for year 6.

Chemical variables show similar undetectable relationships with age, at least with the tests run for this study. Scatterplots have shallow slopes, high variability, and poor correlations (fig. 11). Some of the detected trends were counterintuitive; N and CNRATIO, for example, increased and decreased with age, respectively, when we know that decomposition often results in decreased nitrogen concentrations. All Kendall's Tau values for the chemical variables were less than 0.20 for age. Furthermore, none of the spatial statistics computed from the semivariogram analysis was correlated with age (fig. 12).

Results from our paired site analysis to detect changes in fuel properties within sites that had the same climate and mastication method show that many fuel characteristics changed with age, but the high variation within sites often overwhelmed detection of statistical significance (table 19). Only CNRATIO and N had significant changes across all three paired sites. Values for the loading variables DLOAD and S1LOAD (1-hr fuels) were significantly lower in the older units for the Valles Caldera site. The variables MC and C were significantly different only at the Amber sites. PD was significantly different at the Amber and LG and PAL paired sites. WIDTH showed a significant difference between the Valles Caldera sites, and SAVR showed a significant difference at the paired LG and PAL and Valles Caldera sites.
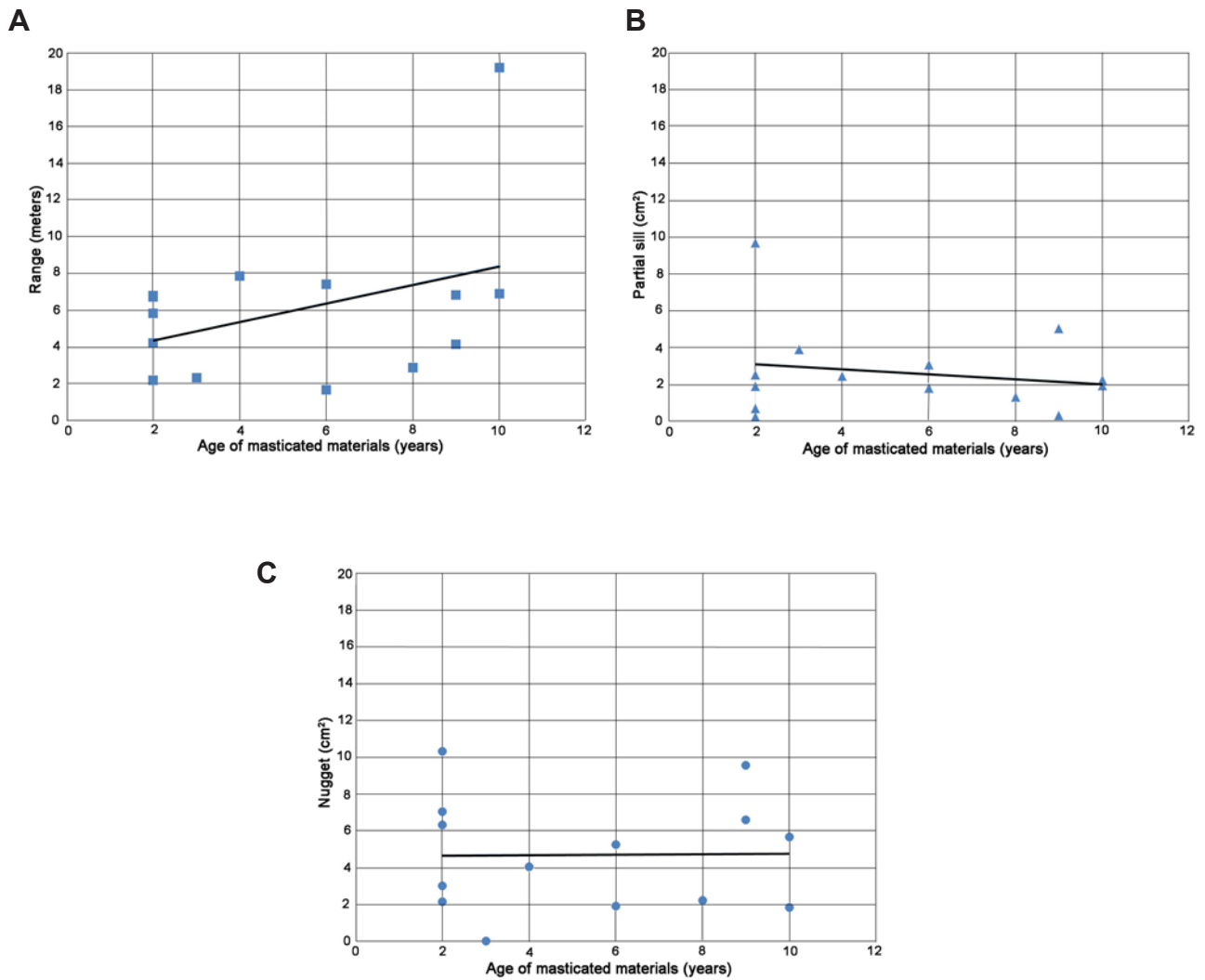
3.3.3 Other Relationships

The strongest relationships occurred when the loading, physical, and chemical characteristics were related to the mastication treatment type (table 18; fig. 13), but these differences were still overwhelmed by the great variability in values for fuel properties. Results from the Freidman analysis (table 18) show many variables differ by mastication method (MAST), including WIDTH, HC, LIG, DBULK, S100LOAD, CELL, S1LOAD, and DLOAD (pval < 0.05). This finding is described in detail in another MASTIDON report in preparation and will not be detailed here.

Site type (xeric vs. mesic; CLIMATE) was also important in the analysis (table 18, fig. 14). Most of the loading variables (TLOAD, DLOAD, and MLOAD) and bulk densities (BD, LBULK, MBULK, and DBULK) were significantly different across dry and moist sites (pval < 0.05). Particle density was also significant. However, many of the measured variables for both CLIMATE and MAST were not significantly different across the categories.
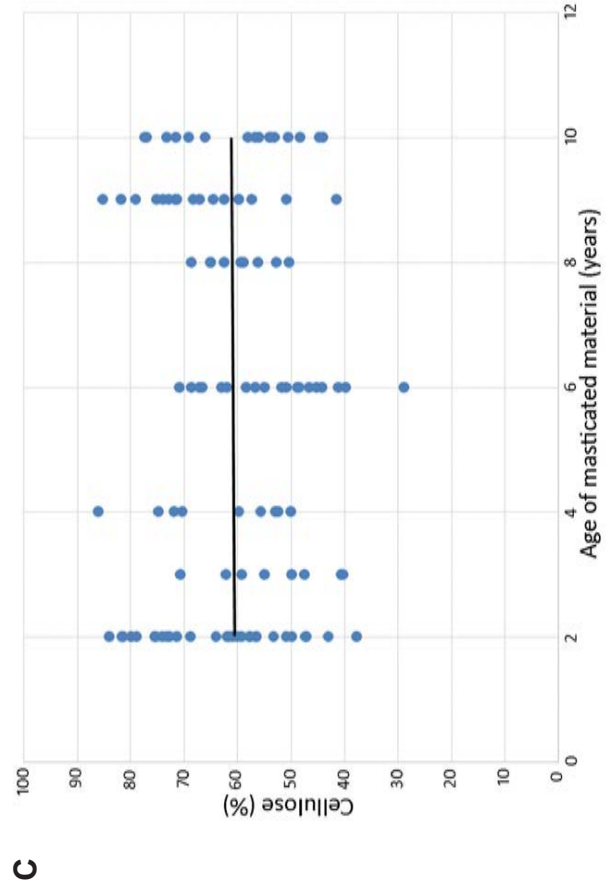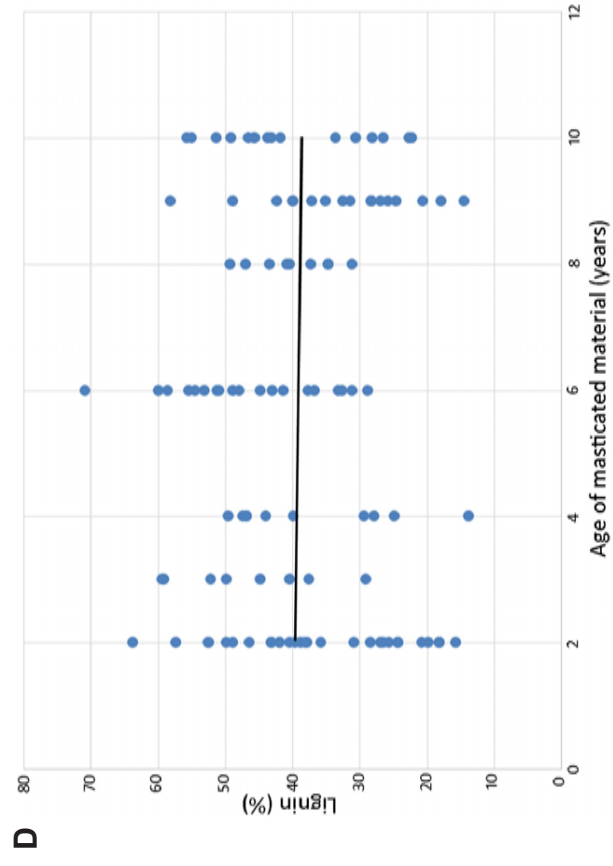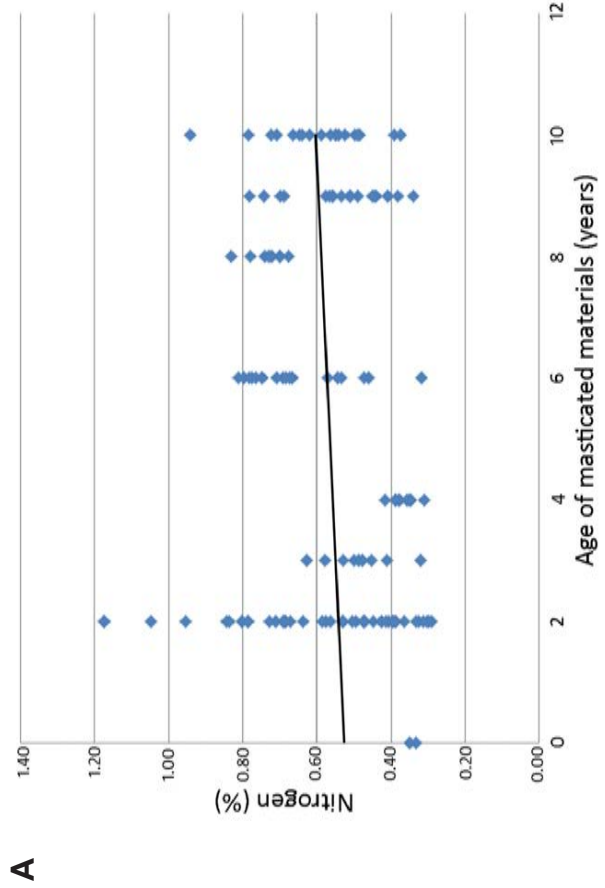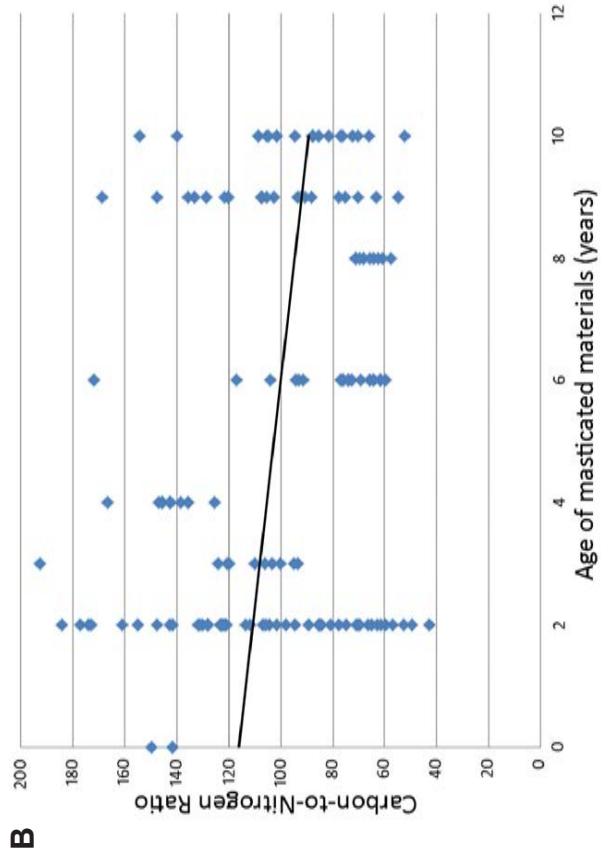
Figure 11—The four chemical variables with the most significant correlation with treatment age (time since treatment): (a) nitrogen, (b) carbon:nitrogen ratio, (b) cellulose + hemicellulose proportion, and (d) lignin proportion. Linear trend lines shown. Graphs based on average values from 151 microplots.

Figure 12—The relationship of the (a) range, (b) partial sill, and (c) nugget to age of masticated fuels for 14 of the 15 sites in the study. Linear trend line shown. Each marker represents the average of 150 to 195 sample points per location.

Table 19—Median values for fuel property characteristics across paired sites that are adjacent to each other and have the same mastication method treatment. Statistically significant differences at the level of $P < 0.05$ using the Mann-Whitney Ranked Sign Test for paired values are highlighted in gray. Site codes are defined in table 4 and variables are defined in table 6.

Variable	Units	Paired Masticated Sites					
		Amber	Amber New	LG	PAL	VC1	VC2
Treatment year	Year	2004	2010	2006	2012	2007	2012
LLOAD	kg m^{-2}	1.09	1.18	0.58	0.41	0.59	1.12
MLOAD	kg m^{-2}	1.38	2.20	2.74	2.91	5.37	3.30
DLOAD	kg m^{-2}	0.43	0.50	3.85	3.41	3.01	1.54
TLOAD	kg m^{-2}	3.05	4.08	8.27	7.24	8.52	6.32
S1LOAD	kg m^{-2}	0.11	0.18	0.41	0.24	0.74	0.15
S10LOAD	kg m^{-2}	0.65	0.69	1.09	1.18	1.87	1.02
S100LOAD	kg m^{-2}	0.31	0.74	0.67	0.73	1.35	1.38
LBULK	kg m^{-3}	44.77	34.01	29.05	61.10	24.29	44.39
MBULK	kg m^{-3}	98.62	87.08	162.60	120.50	144.02	112.87
DBULK	kg m^{-3}	18.76	27.15	119.44	91.95	84.43	76.00
BD	kg m^{-3}	44.71	58.50	99.18	101.01	98.12	91.36
HC	percent	20.21	19.95	19.84	19.83	20.02	19.65
MC	percent	85.68	87.21	88.45	84.78	88.78	91.60
CELL	percent	53.73	57.90	59.50	59.51	56.87	62.16
LIG	percent	45.84	42.10	40.50	40.49	43.13	37.84
N	percent	0.51	0.37	0.73	0.47	0.73	0.43
C	percent	49.41	48.57	46.93	47.60	47.85	49.00
CNRATIO	dim	105.17	142.70	65.63	112.98	67.59	121.88
LENGTH	cm	83.02	90.75	48.12	71.50	50.23	41.28
WIDTH	cm	12.01	10.54	11.34	13.41	12.21	10.58
PD	g cm^{-3}	0.39	0.45	0.35	0.39	0.36	0.38
PW	g	4.43	6.82	2.05	4.52	2.81	2.62
SA	cm^{2}	103.65	76.77	34.44	84.24	36.55	31.05
PV	cm^{3}	12.93	14.33	6.35	11.90	6.75	6.01
SAVR	cm^{-1}	25.48	27.10	15.27	20.61	13.83	18.90
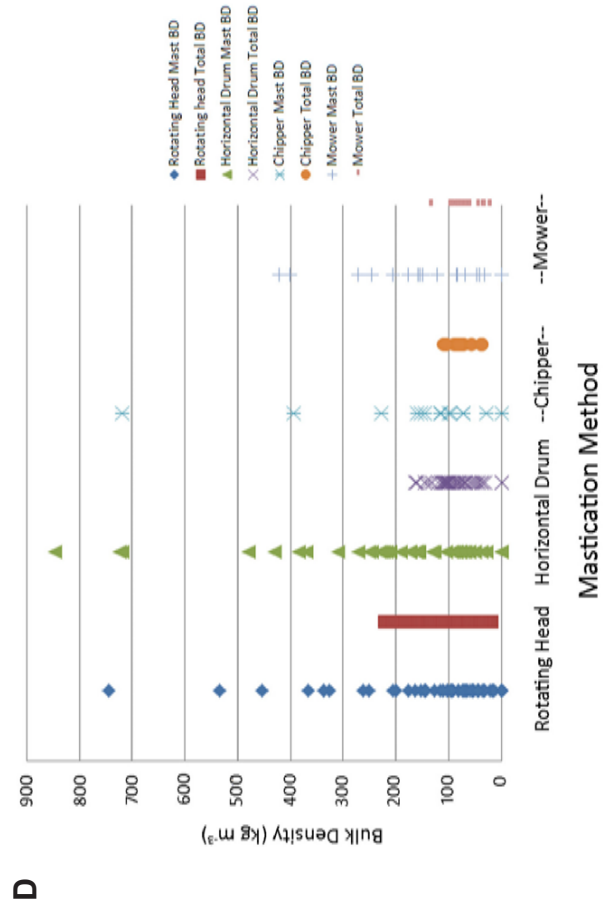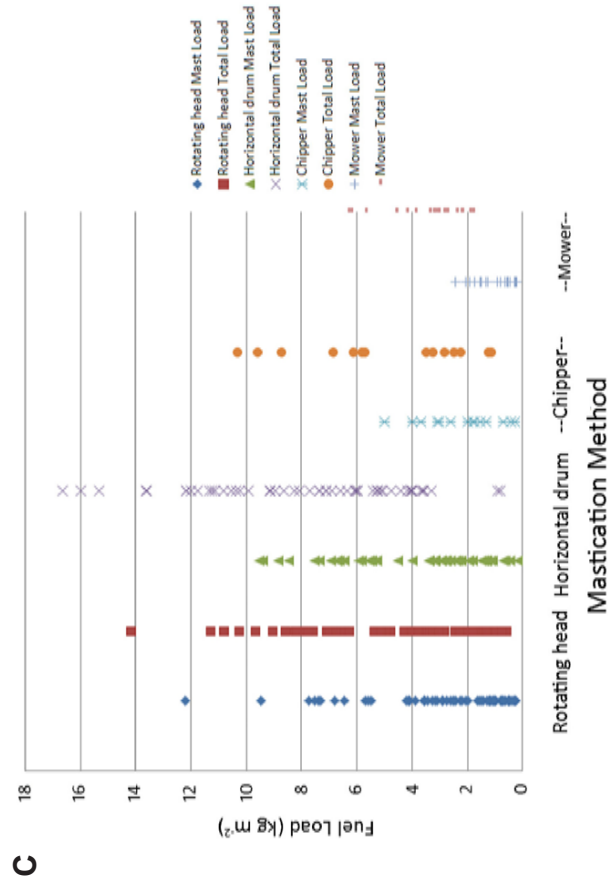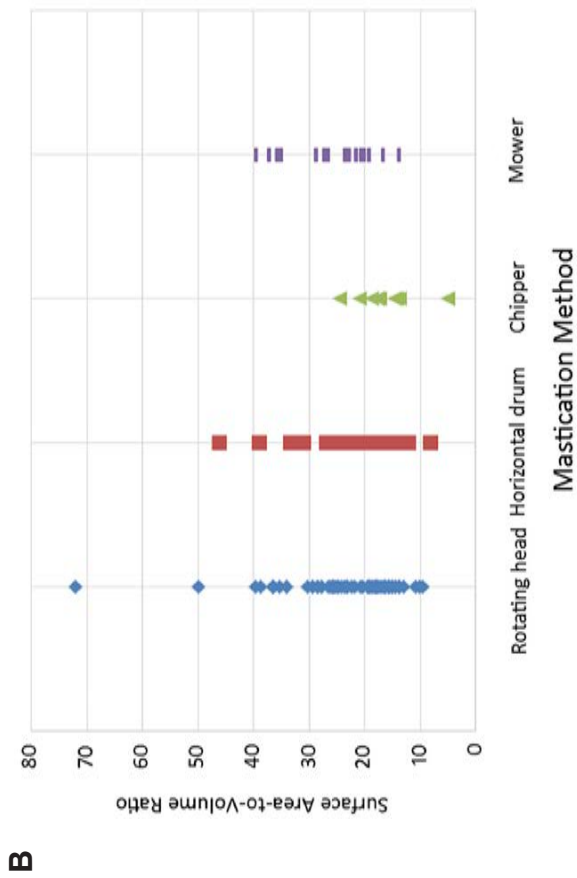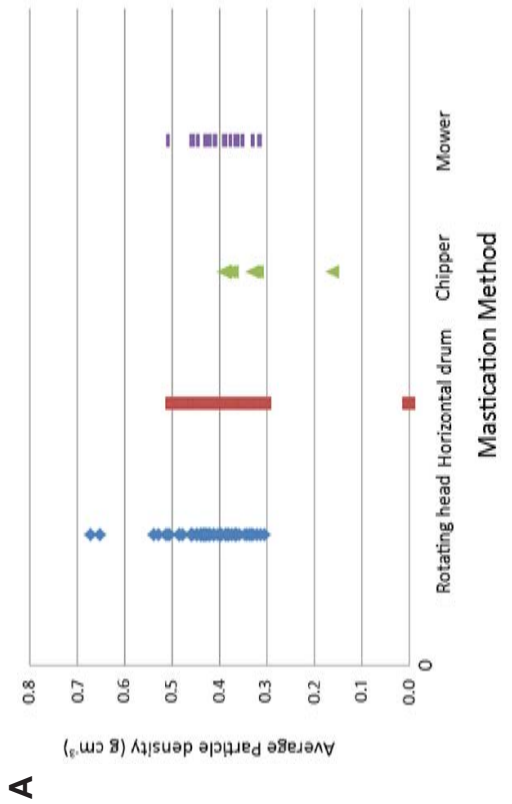
Figure 13—The four loading and physical variables most important to fire behavior prediction summarized by mastication treatment type: (a) particle density, (b) particle surface-area-to-volume ratio, (c) total fuelbed loading, and (d) total fuelbed bulk density. Variables for particles include include ranges for the masticated layer only. Graphs based on average values from 151 microplots.
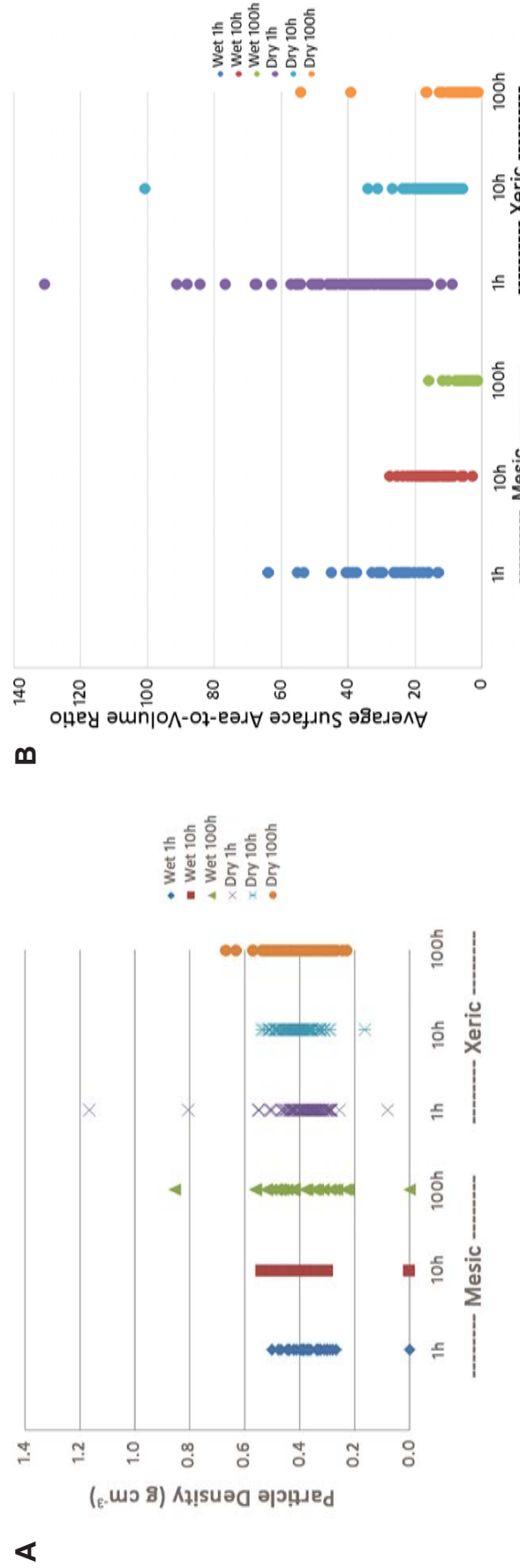
Figure 14—The four loading and physical variables most important to fire behavior prediction summarized by size class and site type (Mesic = moist-northern Idaho sites, Xeric = dry mixed-conifer/ponderosa pine sites): (A) particle density, (b) particle surface-area-to-volume ratio, (c) total fuelbed loading, and (d) total fuelbed bulk density. Graphs based on average values from 151 microplots. Variables for particles include ranges for masticated layer only.

4. Discussion

Our analysis found few changes in most of the measured masticated fuelbed properties over the 10 years represented in our sample. Woody fuel decomposition was expected to alter important physical characteristics, such as particle density, surface area, and bulk density, and the critical chemical properties, primarily nitrogen, lignin, and cellulose + hemicellulose fractions, of masticated fuels (Keane 2015), yet we found few significant changes. The few changes that we observed in our study, such as decreases in nitrogen and cellulose concentrations and increases in bulk density (table 7), were minor and highly variable.

There are probably several reasons that we found little change in fuel properties over a decade. First, most of the sites sampled (11 of 15) were warm, dry mixed-ponderosa pine sites with low precipitation and high temperatures where decomposition was slow. Previous studies in woody fuel decomposition indicated that these warm, dry sites had the lowest decomposition rates of most sites in the Northern Rocky Mountains (Keane 2008a,b). Second, deposition of posttreatment fuels, such as litter and woody debris from surviving trees, may have added newer fuel to aging fuelbeds, thereby influencing physical and chemical characteristics. The study sites also did not have the same silvicultural prescription for cutting trees; the resulting disparate posttreatment tree densities influenced accumulation of woody debris since mastication. Our data were not normally distributed, so we were required to use nonparametric statistics, which have little power and limited ability to detect significant relationships (Boddy and Smith 2009). The main source of variation is in the inherent natural variability of Rocky Mountain fuelbeds. Wildland fuels are notorious variable over space and time (Brown and Bevins 1986; Keane et al. 2012b), and this high natural variability often contributes to low success in detecting statistical differences (Keane 2015).

Another source contributing to high variability is the great differences among mastication techniques (fig. 11). We had to include four mastication methods in the study because it was logistically difficult to get enough sites of different ages by holding mastication method constant. Again, in our pairwise comparison when mastication method is the same across the pair, there were subtle differences with age (table 19). The interaction of mastication method with climate also compounds variability. Techniques that produce smaller, amorphous particles may have decomposed faster, especially on mesic sites; disparate mastication methods across disparate sites increase variability in fuel properties (fig. 3).

However, we feel that the great differences in biophysical conditions across the different aged sites (table 4) added the most variation in our substitute-space-for-time empirical approach. The dry, warm mixed-ponderosa pine sites were scattered over Idaho, Montana, South Dakota, and New Mexico, while the mesic sites were from different stands with different species in a small area of northern Idaho (table 4). Combining these two site types also increased variance and made it difficult to get statistically significant relationships with age. When we excluded mesic sites from the analysis, our correlations increased but only marginally (table 18). However, when we held site and mastication method constant in our paired site comparison (section 3.3.2), we found that there were indeed the anticipated changes occurring over time (table 19).

Other studies have found significant differences in fuel properties over 10 to 16 years, but for different geographical areas and ecosystems. Reed (2015) found changes in particle density and bulk density in shrub woody fuels over time on masticated sites in California and Oregon. Brennan and Keeley (2015) documented changes in cover, depth, and loading of masticated fuelbeds in chaparral ecosystems and found statistically significant relationships with age, but their coefficients of determination (R^2) were similar to our study (<0.34) because, like this study, the variabilities across sites within age classes were very high. Also similar to this study, they found mastication technique significantly important in explaining the high variability across years. Kreye et al. (2016) found that loading actually increased by 2.2 kg m^{-2} from 2 to 16 years old, but bulk densities stayed the same at 82.8 kg m^{-3} (within the range found in this study). Shakespear (2014) found masticated fuels decreased by 0.2 to 0.8 kg m^{-2} within 5 to 6 years (a reduction of about 10 to 80 percent) after treatment, depending on tree cover, in masticated pinyon-juniper (*Pinus edulis/Juniperus* spp.) stands in Utah.

Our measured masticated fuel loadings mostly agreed with other values found in the literature. In a study directly comparable to ours, Battaglia et al. (2010) measured fuel loadings on mulched fuelbeds in Colorado ponderosa pine stands; measured mulched loadings were within 10 percent of the loadings in our masticated ponderosa pine stands. They found most of the mulched fuel in the 10- and 100-hr fuels similar to our results. Glitzenstein et al. (2006) measured loadings in chipped loblolly pine (*Pinus taeda*) flatwoods of South Carolina; their values are well within the range of loadings measured in this study, especially for 1-, 10-, and 100-hr fuels (0.05 to 0.8 kg m^{-2}). However, we found fewer logs on our sites; their log loading exceeded 28.0 kg m^{-2}. A study by Moghaddas and Stephens (2007) found a log loading of more than 2.9 kg m^{-2} on masticated pine sites. These differences are primarily due to different silvicultural prescriptions and harvesting techniques.

Kane et al. (2009) measured loadings of 1.5 to 6.3 kg m^{-2} in masticated shrub and forest fuelbeds in northern California and Oregon. They found most of the woody fuel concentrated in the 1-hr and 10-hr classes (>70 percent) with masticated fuel depths ranging from 4.6 to 8.0 cm, comparable to values measured in this study. Loading measurements in northern California young ponderosa pine forests with shrubs were lower than our study (1.5 to 3.9 kg m^{-2} woody loading) with depths ranging from 5.4 to 12.9 cm (deeper than our study); most of the masticated woody fuel was in the 10-hr size class (Knapp et al. 2011). Our study had lighter loadings than those in a study by Kobziar et al. (2009), who measured nearly double the loadings on a masticated mixed-conifer forest in the Sierra Mountains; their site was more mesic and productive than our ponderosa pine-dominated sites. Reiner et al. (2009) measured loads and depths in a southern Sierra ponderosa pine plantation that were within the range measured in this study. Kane et al. (2006) measured total woody fuel loadings from 1.5 to 6.3 kg m^{-2} in northern California and Oregon with depths of 3.0 to 7.0 cm, and they found most of the woody fuels were in the 10-hr category with little log loading, similar to this study. The range of loadings measured here (table 7) is comparable to all ponderosa pine sites included in a review paper by Kreye et al. (2014a). Duff loadings (0.6 to 4.6 kg m^{-2}) were quite similar to those measured by Kreye et al. (2014b) for pine flatwoods of Florida (1.4 to 9.8 kg m^{-2}).

Some of our physical and chemical fuel properties were also comparable to other studies. In the Kreye et al. (2014a) paper, measured fuelbed bulk densities of 16.7 to

133.0 kg m^{-3} were within the range of this study (52.0 to 102.0 kg m^{-3}) except for the outliers. Reiner et al. (2009) measured bulk densities (12 to 57 kg m^{-3}) that were also similar to our study even though their stand was a ponderosa pine plantation that was only 25 years old. Values for our surface-area-to-volume ratio (SAVR) (17 to 29 cm^{-1}) were close to the SAVR values used by Knapp et al. (2011) in their fuel model construction (24 cm^{-1}). Brewer et al. (2013) measured C:N ratios between 103 and 477 for masticated western white pine and Douglas-fir stands in Idaho, whereas our values ranged from 75 to 160; the disparity could be related to differences in productivity and decomposition rates. Rhoades et al. (2012) also found C:N ratios ranged from 120 to 140 in freshly mulched fuelbeds and from 70 to 85 in old mulch. Our heat content values (18 to 21 MJ kg^{-1}) are slightly lower than those found in the literature: Kelsey et al. (1979) found 20 to 22 MJ kg^{-1}, Van Wagtendonk et al. (1998) found 19 to 22 MJ kg^{-1}, and Susott et al. (1975) found 20 to 22 MJ kg^{-1} for ponderosa pine. These differences could be explained by differences in site and measurement technique.

4.1 Study Limitations

There are many sources of error in this study that may influence interpretation of the results. First, the action of the mastication machinery to mix mineral soil into the duff certainly influenced duff loadings (table 7). The high mineral content of the duff (>80 percent; table 12) partially contributed to higher loadings to create a layer that might be difficult to burn (Philpot 1970). A major reason for these high mineral contents is that we put all unidentifiable material less than 6 mm in diameter, which was mostly finely shredded wood slivers, into the duff for logistical reasons, and most of this material was high in mineral content. We could have reported duff loadings without the mineral fraction but, because of the limited range of mineral content across sites, we doubt it would have affected our findings. The subjective location of the sampling grid (section 2.2) may not be representative of the mastication treatment across a large area. It was also difficult to visually distinguish between the various fuel layers when measuring depths in the field (section 2.2.1) and the collection of masticated material in the 1-m^2 microplot was sometimes difficult because many particles extended beyond the microplot boundaries (section 2.2.2). Sorting was a highly subjective process conducted by multiple lab technicians, potentially adding bias to the measurements. We also excluded logs, shrubs, and herbaceous fuels from this study because they occurred with low frequency in our study sites and were outside the scope of the MASTIDON project. But many masticated sites in the U.S. Rocky Mountains include significant loadings of these fuels, which could influence masticated fuelbed properties and subsequent combustibility. The calculation of surface area (SA) and consequently SAVR used a rather coarse method that computes surface area from standard volume and surface area equations (section 2.3.2.2). Complex shapes and differences in particle dimensions over the length of the particles were often ignored. There are surprisingly few cost-effective alternatives for estimating SA and SAVR. Computation of cellulose + hemicellulose and lignin from heat content may ignore other chemicals in a particle that could contribute to heat content (Van Wagtendonk et al. 1998). Last, as noted earlier, the space-for-time substitution includes additional unexplained variation that may overwhelm age relationships in response variables; it would be far better, but more costly, time-consuming, and prolonged, to measure fuel properties from each site over time (Pickett 1989).

4.2 Management Implications

The primary implication of this study's findings is that masticated fuelbeds, especially in dry environments, may take at least 10 years for ecological processes to change fuel characteristics enough for adverse fire effects to be mitigated. The most harmful impact of mastication occurs when the fuelbed burns in a wildfire because the often prolonged and intense post-frontal combustion period results in deep soil heating and lingering surface heat intensity that tends to kill plants, especially living trees left after mastication (Bradley et al. 2006; Busse et al. 2005; Reiner et al. 2009). Fire managers often hope that masticated fuels will decompose quickly to reduce the adverse effects of prolonged combustion. But this may not be the case for some ponderosa pine-dominated stands, such as the ones in this study, as there were few changes in fuel characteristics with time since treatment for most of our sampled sites. Furthermore, when masticated fuelbeds are burned in wildfires, the subsequent fire effects, such as soil hydrophobicity and plant mortality, may possibly be much greater than if the area had never been masticated.

One common alternative would be to burn these fuelbeds with prescribed fire in moderate weather conditions before the wildfire occurs. However, it may be difficult to design a burn prescription for masticated fuelbeds that would minimize mortality and still reduce hazardous fuel loadings. Sometimes, it might be easier to use prescribed fire to burn the site without a mastication treatment, depending on canopy fuel characteristics. At any rate, the longer the masticated fuelbed remains intact, the higher the potential for unwanted high-severity fire that may cause uncharacteristic severe damage to the stand.

The data summaries presented in this report should have great value to fuel and fire managers. First, many of our measured fuel properties (tables 7, 9, 11) are useful inputs to fire behavior and fire effects models (Andrews 1986; Reinhardt and Keane 1998) and provide the data for developing other fire behavior fuel models (Burgan and Rothermal 1984). Fire managers can use the data presented here to initialize fire models and to parameterize fuel inputs (Knapp et al. 2008). The fuel properties presented here can also be used as inputs to ecosystem models to simulate future decomposition (Keane 2008a). The data may also provide information that is useful for wildlife habitat description (Pilliod et al. 2006; Ucitel et al. 2003), erosion control (Kokaly et al. 2007; Robichaud et al. 2007), and site productivity longevity (Harvey et al. 1989).

5. Conclusion

We found few changes in masticated fuelbed properties over 10 years in the sites represented in this study. This absence of change is most likely due to the naturally high variability of fuel properties and the increased variability introduced in the study when we included sites of different treatment ages across a large geographic area that had been treated by four mastication methods.

6. Literature Cited

Achtemeier, G.L.; Glitzenstein, J.; Naeher, L.P. 2006. Measurements of smoke from chipped and unchipped plots. Southern Journal of Applied Forestry. 30(4): 165–171.

Andrews, P.L. 1986. BEHAVE: Fire behavior prediction and fuel modeling system—BURN subsystem. Gen. Tech. Rep. INT-194. Ogden, UT: U.S. Department of Agriculture, Forest Service, Intermountain Research Station. 130 p.

Battaglia, M.A.; Rhoades, C.; Fornwalt, P.; [et al.]. 2015. Mastication effects on fuels, plants, and soils in four western U.S. ecosystems: Trends with time-since-treatment. Joint Fire Science Final Report, Project 10-1-01-10. Fort Collins, CO: U.S. Department of Agriculture, Forest Service, Rocky Mountain Research Station. 37 p.

Battaglia, M.; Rhoades, C.; Rocca, M.; [et al.]. 2006. A regional assessment of the ecological effects of chipping and mastification fuels reduction and forest restoration treatments. Joint Fire Sciences Program final report. JFSP Research Project Reports. Paper 148. Fort Collins, CO: U.S. Department of Agriculture, Forest Service, Rocky Mountain Research Station. 37 p.

Battaglia, M.A.; Rocca, M.E.; Rhoades, C.C.; [et al.]. 2010. Surface fuel loadings within mulching treatments in Colorado coniferous forests. Forest Ecology and Management. 260(9): 1557–1566. doi: http://dx.doi.org/10.1016/j.foreco.2010.08.004.

Berry, A.H.; Hesseln, H. 2004. The effect of the wildland urban interface on prescribed burning costs in the Pacific Northwestern United States. Journal of Forestry. 102(6): 33–37.

Boddy, R.; Smith, G. 2009. Non-parametric statistics. In: Statistical methods in practice: For scientists and technologists. Hoboken, NJ: John Wiley & Sons, Ltd.: 129–138.

Bradley, T.; Gibson, J.; Bunn, W. 2006. Fire severity and intensity during spring burning in natural and masticated mixed shrub woodlands. In: Fuels management: How to measure success: Conference proceedings; 2006 March 28–30; Portland, OR. Proceedings RMRS-P-41. Fort Collins, CO: U.S.Department of Agriculture, Forest Service Rocky Mountain Research Station: 419–428.

Brennan, T.J.; Keeley, J.E. 2015. Effect of mastication and other mechanical treatments on fuel structure in chaparral. International Journal of Wildland Fire. 24(7): 949–963. doi: http://dx.doi.org/10.1071/WF14140.

Brewer, N.W.; Smith, A.M.S.; Hatten, J.A.; [et al.]. 2013. Fuel moisture influences on fire-altered carbon in masticated fuels: An experimental study. Journal of Geophysical Research: Biogeosciences. 118(1): 30–40. doi: 10.1029/2012jg002079.

Brown, J.K.; Bevins, C.D. 1986. Surface fuel loadings and predicted fire behavior for vegetation types in the northern Rocky Mountains. Res. Note INT-358. Ogden, UT: U.S. Department of Agriculture, Forest Service, Intermountain Research Station. 9 p.

Burgan, R.E.; Rothermal, R.C. 1984. BEHAVE: Fire behavior prediction and fuel modeling system—FUEL subsystem. Gen. Tech.l Rep. INT-167. Ogden, UT: U.S. Department of Agriculture, Forest Service, Intermountain Forest and Range Experiment Station. 126 p.

Busse, M.; Shestak, C.; Knapp, E.; [et al.]. 2006. Lethal soil heating during burning of masticated fuels: Effects of soil moisture and texture. Unpublished paper on file at: U.S. Department of Agriculture, Forest Service, Pacific Southwest Research Station, Albany, CA.

Busse, M.D.; Hubbert, K.R.; Fiddler, G.O.; [et al.]. 2005. Lethal soil temperatures during burning of masticated forest residues. International Journal of Wildland Fire. 14(3): 267–276. doi: http://dx.doi.org/10.1071/WF04062.

Coulter, E.; Coulter, K.; Mason, T. 2002. Dry forest mechanized fuels treatment trials project final report. Central Oregon Intergovernmental Council. 92 p.

Duryea, M.L.; English, R.J.; Hermansen, L.A. 1999. A comparison of landscape mulches: Chemical, allelopathic, and decomposition properties. Journal of Arboriculture. 25(2): 88–97.

ESRI 2014. ArcGIS Desktop: Release 10. Redlands, CA: Environmental Systems Research Institute.

Forests and Rangelands. 2015. Forest operations equipment catalog: Mulchers. Washington, DC: U.S. Department of the Interior and U.S. Department of Agriculture, Forests and Rangelands. https://www.forestsandrangelands.gov/catalog/equipment/mulchers.shtml.

Fortin, M.-J. 1999. Spatial statistics in landscape ecology. In: Klopatek, J.M.; Gardner, R.H., eds. Landscape ecological analysis: Issues and applications. New York: Springer-Verlag, Inc.: 253–279.

Glitzenstein, J.S.; Streng, D.R.; Achtemeier, G.L.; [et al.]. 2006. Fuels and fire behavior in chipped and unchipped plots: Implications for land management near the wildland/urban interface. Forest Ecology and Management. 236(1): 18–29. doi: http://dx.doi.org/10.1016/j.foreco.2006.06.002.

Halbrook, J.; Han, H.-S.; Graham, R.T.; [et al.]. 2006. Mastication: A fuel reduction and site preparation alternative. In: Chung, W.; Han, H.S., eds. Proceedings of the 29th Council on Forest Engineering Conference; 2006 July 30–August 2; Coeur d'Alene, ID. Corvalis, OR: Council on Forest Engineering: 137–146.

Harmon, M.E.; Franklin, J.F.; Swanson, F.J.; [et al.]. 1986. Ecology of coarse woody debris in temperate ecosystems. Advances in Ecological Research. 15: 133–302.

Harrod, R.; Ohlson, P.; Flatten, L.; [et al.]. 2009. A user's guide to thinning with mastication equipment. Wenatchee, WA: U.S. Department of Agriculture, Forest Service, Pacific Northwest Region, Okanogan-Wenatchee National Forest.

Harvey, A.E.; Jurgensen, M.F.; Graham, R.T. 1989. Fire-soil interactions governing site productivity in the northern Rocky Mountains. In: Prescribed fire in the Intermountain Region—Symposium proceedings. Pullman, WA: Washington State University, Cooperative Extension: 9–19.

Hatten, J.A.; Zabowski, D. 2010. Fire severity effects on soil organic matter from a ponderosa pine forest: A laboratory study. International Journal of Wildland Fire. 19(5): 613–623. doi:10.1071/Wf08048.

Hood, S.; Wu, R. 2006. Estimating fuel bed loadings in masticated areas. In: Fuels management: How to measure success: Conference proceedings; 2006 March 28–30; Portland, OR. Proceedings RMRS-P-41. Fort Collins, CO: U.S.Department of Agriculture, Forest Service Rocky Mountain Research Station: 333–345.

Jain, T.B.; Battaglia, M.A.; Han, H.-S.; [et al.]. 2012. A comprehensive guide to fuel management practices for dry mixed conifer forests in the northwestern United States. Gen. Tech. Rep. RMRS-GTR-292. Ogden, UT: U. S. Department of Agriculture, Forest Service, Rocky Mountain Research Station.

Kane, J.M.; Knapp, E.E.; Varner, J.M. 2006. Variability in loading of mechanically masticated fuel beds in northern California and southwestern Oregon. In: Fuels management—How to measure success; Portland, OR USA. Proceedings RMRS-P-41. USDA Forest Service Rocky Mountain Research Station: 341–348.

Kane, J.M.; Varner, J.M.; Knapp, E.E. 2009. Novel fuel characteristics associated with mechanical mastication treatments in northern California and south-western Oregon, USA. International Journal of Wildland Fire. 18: 686–697.

Keane, R.E. 2008a. Biophysical controls on surface fuel litterfall and decomposition in the northern Rocky Mountains, USA. Canadian Journal of Forest Research. 38(6): 1431–1445. doi: 10.1139/X08-003.

Keane, R.E. 2008b. Surface fuel litterfall and decomposition in the northern Rocky Mountains, USA. Res. Pap. RMRS-RP-70. Fort Collins, CO: U.S. Department of Agriculture, Forest Service, Rocky Mountain Research Station. 22 p.

Keane, R.E. 2015. Wildland fuel fundamentals and applications. New York: Springer. 191 p.

Keane, R.; Gray, K.; Bacciu, V.; [et al.]. 2012a. Spatial scaling of wildland fuels for six forest and rangeland ecosystems of the northern Rocky Mountains, USA. Landscape Ecology. 27(8): 1213–1234. doi: 10.1007/s10980-012-9773-9.

Keane, R.E.; Gray, K.; Bacciu, V. 2012b. Spatial variability of wildland fuel characteristics in northern Rocky Mountain ecosystems. Res. Pap. RMRS-RP-98. Fort Collins, CO: U.S. Department of Agriculture Forest Service, Rocky Mountain Research Station. 56 p.

Kelsey, R.G.; Shafizadeh, F.; Lowery, D.P. 1979. Heat content of bark, twigs, and foliage of nine species of western conifers. Res. Note INT-261. Ogden, UT: U.S. Department of Agriculture, Forest Service. Intermountain Forest and Range Experiment Station. 7 p.

Knapp, E.E.; Busse, M.D.; Varner, J.M., III; [et al.]. 2008. Masticated fuel beds: Custom fuel models, fire behavior, and fire effects. Joint Fire Sciences Program Final Report. Project number 05-2-1-20. Redding, CA: U.S. Department of Agriculture, Forest Service, Pacific Southwest Research Station. 17 p.

Knapp, E.E.; Varner, J.M.; Busse, M.D.; [et al.]. 2011. Behaviour and effects of prescribed fire in masticated fuelbeds. International Journal of Wildland Fire. 20(8): 932–945. doi: http://dx.doi.org/10.1071/WF10110.

Kobziar, L.N.; McBride, J.R.; Stephens, S.L. 2009. The efficacy of fire and fuels reduction treatments in a Sierra Nevada pine plantation. International Journal of Wildland Fire. 18(7): 791–801. doi: http://dx.doi.org/10.1071/WF06097.

Kokaly, R.F.; Rockwell, B.W.; Haire, S.L.; [et al.]. 2007. Characterization of post-fire surface cover, soils, and burn severity at the Cerro Grande Fire, New Mexico, using hyperspectral and multispectral remote sensing. Remote Sensing of Environment. 106(3): 305–325. doi: 10.1016/j.rse.2006.08.006.

Kreye, J.; Varner, J. 2007. Moisture dynamics in masticated fuelbeds: A preliminary analysis. In: Butler, Bret W.; Cook, Wayne, eds. The fire environment—Innovations, management, and policy; conference proceedings. Proceedings RMRS-P-46CD. Fort Collins, CO: U.S. Department of Agriculture, Forest Service, Rocky Mountain Research Station: 173–186.

Kreye, J.K.; Brewer, N.W.; Morgan, P.; [et al.]. 2014a. Fire behavior in masticated fuels: A review. Forest Ecology and Management. 314(0): 193–207. doi: http://dx.doi.org/10.1016/j.foreco.2013.11.035.

Kreye, J.K.; Kobziar, L.N.; Camp, J.M. 2014b. Immediate and short-term response of understory fuels following mechanical mastication in a pine flatwoods site of Florida, USA. Forest Ecology and Management. 313(0): 340–354. doi: http://dx.doi.org/10.1016/j.foreco.2013.10.034.

Kreye, J.K.; Varner, J.M.; Kane, J.M.; [et al.]. 2016. The impact of aging on laboratory fire behaviour in masticated shrub fuelbeds of California and Oregon, USA. International Journal of Wildland Fire. 25(9): 1002–1008. doi: http://dx.doi.org/10.1071/WF15214.

Kreye, J.K.; Varner, J.M.; Knapp, E.E. 2012. Moisture desorption in mechanically masticated fuels: Effects of particle fracturing and fuelbed compaction. International Journal of Wildland Fire. 21(7): 894–904. doi: http://dx.doi.org/10.1071/WF11077.

Lambert, M.B.; McCleese, W.L. 1977. The San Dimas forestland residue machine. Fire Management Notes. Summer: 3–6.

Lutes, D.C.; Benson, N.C.; Keifer, M.; [et al.]. 2009. FFI: A software tool for ecological monitoring. International Journal of Wildland Fire. 18(3): 310–314. doi: http://dx.doi.org/10.1071/WF08083.

Lyon, Z.D. 2015. Fire behavior in masticated forest fuels: Lab and prescribed burn experiments. Thesis. Moscow, ID: University of Idaho.

Math.com. [n.d.]. Volume formulas. Math.com: The World of Math Online. http://www.math.com/tables/geometry/volumes.htm [Accessed October 2014].

McKenzie, D.W.; Makel, B. 1991. Update: Field equipment for precommercial thinning and slash treatment. San Dimas, CA: U.S. Department of Agriculture, Forest Service, San Dimas Technology and Development Center. 69 p.

Moghaddas, E.E.Y.; Stephens, S.L. 2007. Thinning, burning, and thin-burn fuel treatment effects on soil properties in a Sierra Nevada mixed-conifer forest. Forest Ecology and Management. 250(3): 156–166. doi: http://dx.doi.org/10.1016/j.foreco.2007.05.011.

Moreno-Fernández, D.; Hernández, L.; Sánchez-González, M.; [et al.]. 2016. Space-time modeling of changes in the abundance and distribution of tree species. Forest Ecology and Management. 372: 206–216. doi: http://dx.doi.org/10.1016/j.foreco.2016.04.024.

Naeher, L.P.; Achtemeier, G.L.; Glitzenstein, J.S.; [et al.]. 2006. Real-time and time-integrated PM2.5 and CO from prescribed burns in chipped and non-chipped plots: Firefighter and community exposure and health implications. Journal of Exposure Science and Environmental Epidemiology. 16(4): 351–361.

Pan, Y.; Birdsey, R.A.; Fang, J.; [et al.]. 2011. A large and persistent carbon sink in the world's forests. Science. 333(6045): 988–993.

Philpot, C.W. 1970. Influence of mineral content on the pyrolysis of plant materials. Forest Science. 16(4): 461–471.

Pickett, S.T.A. 1989. Space-for-time substitution as an alternative to long-term studies. In: Likens, G.E., ed. Long-term studies in ecology: Approaches and alternatives. New York: Springer-Verlag: 110–135.

Pilliod, D.S.; Bull, E.L.; Hayes, J.L.; [et al.]. 2006. Wildlife and invertebrate response to fuel reduction treatments in dry coniferous forests of the Western United States: A synthesis. Gen. Tech. Rep. RMRS-GTR-173. Fort Collins, CO: U.S. Department of Agriculture, Forest Service, Rocky Mountain Research Station. 34 p.

Pokela, R.W. 1972. Rolling chopper disposes of pine slash. Fire Control Notes. 33(2): 7–8.

R Core Team. 2015. R: A language and environment for statistical computing. Vienna, Austria: R Foundation for Statistical Computing. ISBN 3-900051-07-0. http://www.R-project.org/.

Reed, W. 2015. Long-term fuel and vegetation responses to mechanical mastication. Thesis. Blacksburg, VA: Virginia Polytechnic Institute and State University. 34 p.

Reiner, A.L.; Vaillant, N.M.; Fites-Kaufman, J.; [et al.]. 2009. Mastication and prescribed fire impacts on fuels in a 25-year old ponderosa pine plantation, southern Sierra Nevada. Forest Ecology and Management. 258(11): 2365–2372. doi: http://dx.doi.org/10.1016/j.foreco.2009.07.050.

Reinhardt, E.; Keane, R.E. 1998. FOFEM—A first order fire effects model. Fire Management Notes. 58(2): 25–28.

Rhoades, C.C.; Battaglia, M.A.; Rocca, M.E.; [et al.]. 2012. Short- and medium-term effects of fuel reduction mulch treatments on soil nitrogen availability in Colorado conifer forests. Forest Ecology and Management. 276: 231–238. doi: http://dx.doi.org/10.1016/j.foreco.2012.03.028.

Ritter, E. 1950. Mechanical fire hazard reducer. Fire Control Notes. 11(2): 30–31.

Robichaud, P.R.; Elliot, W.J.; Pierson, F.B.; [et al.]. 2007. Predicting postfire erosion and mitigation effectiveness with a web-based probabilistic erosion model. CATENA. 71(2): 229–241.

Rothermel, R.C. 1972. A mathematical model for predicting fire spread in wildland fuels. Res. Pap. INT-115. Ogden, UT: U.S. Department of Agriculture, Forest Service, Intermountain Research Station. 40 p.

Rummer, R. 2009. New technology in forest operations, Forest Landowner. (January/February): http://c.ymcdn.com/sites/www.forestlandowners.com/resource/resmgr/imported/JF09_New_Technology_in_Forest_Operations.pdf. www.forestlandowners.com (accessed October 2015).

Rummer, R.B. 2006. Mechanical tools for fuels management [Draft]. Chapter 4. In: Cumulative watershed effects of fuels management: A western synthesis: 45–67.

Sarli, G.O.; Filgueira, R.R.; Gimenez, D. 2001. Measurement of soil aggregate density by volume displacement in two non-mixing liquids. Soil Science Society of America Journal. 65: 1400–1403.

Scott, J.; Burgan, R.E. 2005. A new set of standard fire behavior fuel models for use with Rothermel's surface fire spread model. Gen. Tech. Rep. RMRS-GTR-153. Fort Collins, CO: U.S. Department of Agriculture, Forest Service, Rocky Mountain Research Station. 72 p.

Shakespear, A.W. 2014. Fuel response to mechanical mastication of pinyon-juniper woodlands in Utah. Theses. Paper 4317. Provo, UT: Brigham Young University. 53 p.

Sikkink, Pamela G.; Jain, Theresa B.; Reardon, James; [et al.]. 2017. Effect of particle aging on chemical characteristics, smoldering, and fire behavior in mixed-conifer masticated fuel. Forest Ecology and Management. 405: 150–165.

Smith, A.M.S.; Brewer, N.W. 2011. Masticated fuels and carbon storage: Effects of particle size and fuel moisture on black carbon production. JFSP Project Number 11-3-1-30. Final Report. Joint Fire Sciences Program. Moscow, ID: University of Idaho, Department of Forest, Rangeland, and Fire Sciences. 14 p.

Sokal, R.R.; Rohlf, F.J. 1981. Biometry. San Francisco, CA: W.H. Freeman and Company. 859 p.

Stephens, S.L.; McIver, J.D.; Boerner, R.E.; [et al.]. 2012. The effects of forest fuel-reduction treatments in the United States. BioScience. 62(6): 549–560.

Susott, R.A.; DeGroot, W.F.; Shafizadeh, F. 1975. Heat content of natural fuels. Journal of Fire and Flammability. 6: 311–325.

Ucitel, D.; Christian, D.P.; Graham, J.M. 2003. Vole use of coarse woody debris and implications for habitat and fuel management. The Journal of Wildlife Management. 67(1): 65–72.

Van Wagtendonk, J.W.; Sydoriak, W.M.; Benedict, J.M. 1998. Heat content variation of Sierra Nevada conifers. International Journal of Wildland Fire. 8(3): 147–158. doi: doi:10.1071/WF9980147.

Vitorelo, B.; Han, H.-S.H.; Varner, J.M. 2009. Masticators for fuel reduction treatment: Equipment options, effectiveness, costs, and environmental impacts. In: Environmentally sound forest operations; conference proceedings; 2009 June 15–18; Lake Tahoe, CA. Corvalis, OR: Council on Forest Engineering. 11 p.

Weed, A.S.; Bentz, B.J.; Ayres, M.P.; [et al.]. 2015. Geographically variable response of Dendroctonus ponderosae to winter warming in the western United States. Landscape Ecology. 30(6): 1075–1093. doi: 10.1007/s10980-015-0170-z.

Williamson, G.B.; Wiemann, M.C. 2010. Measuring wood specific gravity…correctly. American Journal of Botany. 97(3): 519–524. doi: 10.3732/ajb.0900243.

Windell, J.T.; Willard, B.E.; Cooper, D.J.; [et al.]. 1986. An ecological characterization of Rocky Mountain montane and subalpine wetlands. Washington, DC: U.S. Department of the Interior, Fish and Wildlife Service. 298 p.

Windell, K.; Bradshaw, S. 2000. Understory biomass reduction methods and equipment catalog. Missoula, MT: U.S. Department of Agriculture, Forest Service, Missoula Technology and Development Center. 156 p.